

**Anti-slug control of two-phase flow in risers with:  
Controllability analysis using alternative measurements**

**by**

**Anette Hoel Helgesen**

***SPECIALIZATION PROJECT 2010***

*TKP4550 Process Systems Engineering*

*NTNU*

*10.12.2010*

## Abstract

Riser slugging is a problem in multiphase pipeline systems. Slugging is a flow regime that causes a lot of problems, due to rapid changes in gas and liquid rates entering the separators and large variations in system pressure. Solutions to avoid these slugs are economically feasible and under continuous research. Slug control solution has become an important topic in recent decades. Different control design based on single or multiple measurements can be used for stabilizing control to counteract slugging. A controllability analysis was performed in order to investigate which measurements that are most suited for stabilizing control, and this analysis can be used on both SISO and MIMO systems. A linear model was used to perform analysis, and the model used was a simple low-order dynamical model for severe slugging in pipeline-riser systems. This analysis use the lower bounds on the closed-loop transfer functions  $S$ ,  $T$ ,  $KS$ ,  $SG$ ,  $KSG_d$  and  $SG_d$  to obtain information about achievable performance and possible robustness problems. The peak values for the closed-loop transfer functions were evaluated. Topside pressure should not be used for stabilizing control because of high peak values on all transfer functions. This is due to its RHP-zeros. These RHP-zeros, in combination with RHP-poles, time delays, disturbances, noise and inputs constraints will give limitations in stabilizing control. Inlet pressure has proved to effectively stabilize flow, but unfortunately this subsea measurement is not always available. A difficult task would then be to find other control solutions that use more available measurements and achieve equal results. A combination of topside pressure and volumetric flow rate as measurements is a conclusive solution. As flow measurements should not be used in single-loop stabilizing control, due to low steady-state gain that results in low-frequency performance.

Different control designs were tested in Simulink, on both linear and nonlinear model. Single-loop PI control based on inlet pressure as measurement, managed to stabilize the system quickly after remarkable change in one disturbance when  $Z > 10\%$ . A PI controller based on volumetric flow rate did also stabilize the system, but response was slow and new disturbances probably occur prior to system stabilization. Topside pressure as measurement was unable to stabilize the system when a single-loop PI controller was used. A Kalman filter based on topside pressure and topside flow rate was used to estimate inlet pressure. These estimated values were used as measurements in a single-loop PI controller. It proved impossible to stabilize the flow when this control solution was used. LQG controller with only proportional action based on both single and multiple measurements was tested. A LQG controller based on topside pressure and volumetric flow rate managed to stabilize the linear model and nonlinear model. Deviations between real and estimated values occur, and deviations are largest when LQG control was used on the nonlinear model. There was also a steady state offset when LQG control with only proportional action was used.

## **Acknowledgement**

This is the report for my final year specialization project at Norwegian University of Science and Technology (NTNU). The project has been carried out at the Department of Chemical Engineering and is a part of my Master's degree. The problem formulation has been formulated by Professor Sigurd Skogestad. The project has given me a better understanding of riser slugging and the problems that it make in the oil industry. I have had a great learning profit and I am sure that I will benefit of this work in the future.

I would like to thank my supervisor for this project, Professor Sigurd Skogestad at the Process System Engineering group at NTNU. He has been supporting and given me great ideas trough the whole project. Sigurd has also always taken time to answer my questions and has been positive. I have learned from the best in this project and that I am great full for. Second I would like to thank my co supervisor Esmail Jahanshahi, for his continuous support and enthusiasm. He has been patient, positive and taken time to teach me about his work.

Finally I would like to thank my fellow students for keeping a good spirit and positive atmosphere at our office. But I will also thank the rest of the Process System Engineering group, for good cake and for everybody being so nice and friendly.

# Contents

<b>1</b>	<b>Introduction</b>	<b>1</b>
<b>2</b>	<b>Background</b>	<b>2</b>
2.1	Multiphase flow . . . . .	2
2.2	Riser slugging . . . . .	2
2.2.1	Different slug flows . . . . .	2
2.3	Simplified model . . . . .	4
<b>3</b>	<b>Simulation in OLGA and bifurcation diagrams</b>	<b>6</b>
3.1	Bifurcation diagrams . . . . .	6
<b>4</b>	<b>Controllability analysis of two-phase pipeline-riser system</b>	<b>9</b>
4.1	Linearization . . . . .	9
4.2	Scaling the system . . . . .	10
4.3	Controllability analysis: Theoretical background . . . . .	11
4.3.1	Minimum peaks on $S$ and $T$ . . . . .	13
4.3.2	Minimum peaks on $KS$ . . . . .	14
4.3.3	Minimum peaks on $KSG_d$ . . . . .	14
4.3.4	Minimum peaks on $SG$ . . . . .	15
4.3.5	Minimum peaks on $SG_d$ . . . . .	15
4.3.6	Comment . . . . .	16
4.4	Results and discussion of controllability analysis . . . . .	16
4.4.1	Minimum peaks for different closed-loop transfer functions . . . . .	17
4.4.2	Discussion: Controllability analysis . . . . .	19
4.4.3	Controllability analysis of inlet pressure control . . . . .	20
4.4.4	Controllability analysis of flow control . . . . .	20
<b>5</b>	<b>Controllability analysis on a three state model</b>	<b>22</b>
<b>6</b>	<b>Anti-slug control of two-phase flow in riser and limitations in system</b>	<b>24</b>
6.1	Anti-slug control . . . . .	24
6.2	Limitations in system . . . . .	25
6.2.1	Limitations imposed by inputs . . . . .	25
6.2.2	Limitations imposed by RHP-zeros . . . . .	25
6.2.3	Limitations imposed by time delay . . . . .	26
6.2.4	Limitations imposed by RHP-poles . . . . .	27
6.2.5	Performance requirements imposed by disturbances . . . . .	27
6.3	Anti-slug control of two-phase flow in riser . . . . .	28
6.3.1	Single-loop stabilizing control . . . . .	28
6.3.2	Kalman filter . . . . .	30
6.3.3	Kalman filter and PI controller . . . . .	33
6.3.4	Linear-quadratic regulator (LQG) . . . . .	33
6.4	Previous controller methods used on riser slugging . . . . .	36

<b>7 Conclusion and further work</b>	<b>38</b>
7.1 Conclusion . . . . .	38
7.2 Further work . . . . .	39
<b>Reference</b>	<b>i</b>
<b>A Nomenclature</b>	<b>ii</b>
<b>B The new model</b>	<b>iv</b>
B.1 State equations . . . . .	iv
B.2 Boundary Conditions . . . . .	iv
B.3 Pipeline model . . . . .	v
B.4 Riser model . . . . .	vi
B.5 Model for the gas flow in the low point . . . . .	vii
B.6 Model for the liquid flow in the low point . . . . .	viii
B.7 Phase distribution model at outlet choke valve . . . . .	viii
<b>C Steady state gain</b>	<b>x</b>
<b>D Kalman filter</b>	<b>xi</b>
D.1 Kalman filter in Simulink . . . . .	xii
<b>E Matlab files</b>	<b>xiii</b>
E.1 Controllability analysis: Method 1 . . . . .	xiii
E.2 Controllability analysis: Method 2 . . . . .	xvi
E.2.1 Stable phase, minimum phase and minimum stable phase for $G_i$ transfer functions . . . . .	xxvi
E.2.2 Stable phase, minimum phase and minimum stable phase $G_{d,ij}$ transfer functions . . . . .	xxvi
E.3 LQG controller . . . . .	xxvii
<b>F Risk evaluation</b>	<b>xxviii</b>

## List of Tables

4.1	Topside pressure: Zeros and Poles . . . . .	11
4.2	Results from method 1 . . . . .	17
4.3	Results from method 2 . . . . .	18
5.1	Topside pressure: Zeros and poles . . . . .	22
5.2	Results from method 1 and method 2, $Z=15\%$ . . . . .	23
5.3	Results from method 1 and method 2, $Z=30\%$ . . . . .	23
6.1	Time delays for three measurements . . . . .	26
A.1	Nomenclature . . . . .	ii
C.1	Steady state gain . . . . .	x
E.1	List of MATLAB Files . . . . .	xiii

## List of Figures

2.1	Illustration of the riser slugging in pipeline-riser systems [1] . . . . .	3
3.1	Illustration of the riser model with geometry . . . . .	6
3.2	Bifurcation diagrams . . . . .	7
3.3	Simulation results from OLGA . . . . .	7
4.1	Frequency dependent gain for $P_1$ at operating point $Z=10\%$ and $Z=30\%$ . . . . .	20
4.2	Frequency dependent gain for $Q$ and $W$ at operating point $Z=10\%$ . . . . .	21
6.1	Peak values for $ S $ , with topside pressure as measurement . . . . .	26
6.2	Stabilizing control on linear and nonlinear model, $P_1$ as measurements and $Z=10\%$ . . . . .	29
6.3	Stabilizing control on linear and nonlinear model, $Q$ as measurements and $Z=10\%$ . . . . .	29
6.4	Estimation of $P_1$ , with and $Z=3\%$ . . . . .	30
6.5	Estimation of states, $Z=10\%$ . . . . .	31
6.6	Real and estimated value for $P_1$ , $P_2$ and $Q$ , and deviation . . . . .	32
6.7	Illustration of the setup of a LQG controller[2] . . . . .	34
6.8	LQG controller based on measurement $P_2$ and $Q$ , used on nonlinear model . . . . .	35
6.9	LQG controller based on measurement $P_1$ and $Q$ , used on nonlinear model . . . . .	36
6.10	General control configuration[3] . . . . .	37
D.1	Illustration of the Kalman filter . . . . .	xii
D.2	Kalman filter in Simulink . . . . .	xii

## List of Abbreviations

<b>LHP</b>	Left hand plan
<b>LQG</b>	Linear Quadratic Gaussian
<b>MIMO</b>	Multi-input-multi-output systems
<b>MPC</b>	Model predictive control
<b>NMPC</b>	Nonlinear model predicitive control
<b>P</b>	Proportional (controller)
<b>PI</b>	Proportional-integral (controller)
<b>PID</b>	Proportional-integral-derivative (controller)
<b>RHP</b>	Right hand plan
<b>SIMO</b>	Single-input-multi-output system
<b>SISO</b>	Single-input-single-output systems

# 1 Introduction

Multiphase flow and its behavior has been a concern in offshore oil and gas industry, since start of production. Time, effort and resources have been spent to study this phenomenon. The reason for this concern is that relatively small changes in operating conditions, can change the flow behavior in the pipelines drastically [4]. In oil industry multiphase pipelines are used to connect subsea wells to platforms. Transporting multiphase mixture over long distances, handling of physical flow-impeding phenomena such as slug flow is required [2]. Slug flow is a flow regime in multiphase pipelines that is characterized by irregular flows. Pipeline riser-slugging reduces the production rate, and therefore a solution that guarantee stable flow and maximum production rate is desirable. Reducing the choke valve opening at the topside of the riser (choking) is the conventional solution for avoiding slugging, but stabilizing control system is also a solution of great interest. This is both interesting and challenging, because riser slugging system contains conflicting controllability limitations. Control systems that are designed to avoid riser slugging, are called slug controllers. Different controller designs can be used, with the topside choke used as the manipulated variable. Different measurements are often available, but some of them are less suited to be used for stabilizing control. To find which measurement most suited to use, a controllability analysis can be performed. This analysis can be performed on both SISO and MIMO system.

The goal for this project was to use a simplified dynamic model for severe slugging in pipeline-riser systems, and perform a controllability analysis and use slug-control to avoid riser slugging. The simplified model is a nonlinear mathematical model which has been linearized and scaled before use. Analysis was done in MATLAB for different operating points, and minimum peaks for the different closed-loop transfer functions  $S$ ,  $T$ ,  $KS$ ,  $SG$ ,  $KSG_d$  and  $SG_d$ , were found. Controllability analysis gave which of the measurements that are most suited for stabilizing control. It was attempted to control the system using the results from the analysis, to verify them. First a single-loop PI controller based on different measurement was tested. Second a Kalman filter combined with PI controller was tested, as estimated values for inlet pressure are more readily available than the measured values. At last a LQG controller was used, and two cases were considered; LQG controller based on either topside pressure only or a combination of topside pressure and flow rate. The Kalman filter used was based on a linear model.

## **2 Background**

This is a brief introduction to multiphase flow and what riser slugging is. As there are different types of slug flows, these will also be explained. The goal for this project is to avoid slugging with the use of stabilizing controller systems. Other ways to avoid slugging is available and will be mentioned. By using simple models, different aspect of riser slugging and the change of slug flow regime to a stable regime can be study. Five simplified dynamical models are found in the literature and in this report a model made by Esmail Jahanshahi is used [5]. References to more extensive descriptions and studies are given.

### **2.1 Multiphase flow**

Multiphase flows in subsea pipelines are important in oil and gas industry. Multiphase flow is a term used to refer to any fluid flow consisting of more than one phase or component. In almost all process technology multiphase flow exist, from caviating pumps and turbines to the pellet form of almost all raw plastics. The ability to predict the fluid flow behavior of the multiphase process or flow is central to the efficiency and effectiveness of the process. Flow can be arrange into different configurations and this give different flow regimes or flow patterns. Different intermediate flow patterns can also be present in pipelines. Slug flow is one of these and can occur on different time- and length scale depending on the underlying mechanism for the slug flow formation. Throughout study of multiphase flow, models are needed and predictions of the detailed behavior of these flows and the phenomena that they manifest. There are three ways to find these models. The first one is experimentally by using laboratory-sized models equipped with appropriate instrumentation. The second on is from theory; mathematical equations and models for the flow. The third way is in the use of computers to address the complexity of the flow. [6]

### **2.2 Riser slugging**

As already mentioned, some operating conditions in the multiphase flow can lead to an undesirable slug flow regime. This may cause many problems for a receiving facility [4]. Riser slugging, that is a highly transient flow regime, develops in pipelines from wellheads to separation tanks. These slugs cause oscillations of pressure and flow rates in the process [7]. Being able to avoid slug flow in the pipeline is of great economic interest. To avoid these slugs it is important to predict the flow regime prior to production, in this way problems can be taken care of as soon as they occur [4].

#### **2.2.1 Different slug flows**

There are different types of slug flow and what type it is, depends on formation. Slugs can be caused by hydro-dynamical- or terrain effects [4]. They can also occur because of transient effects related to pigging, start-up and blow-down, and changes in pressure or flow rates. Hydrodynamic slugs are formed from liquid waves grow in the pipeline. These waves grow until the height of the waves is sufficient to completely fill the pipe. Small slugs can join and form larger slugs. These can occur over a wide range of flow conditions. The hydrodynamic slugs are induced by the velocity difference between gas and liquid phase [8]. Terrain slugging is caused by the pipeline geometry, as a result of the low point in the pipeline. In this slugging liquid blocks the gas until the pressure in the compressed gas is large enough to overcome hydrostatic head of the liquid. A liquid slug is then pushed in front of the expanding gas upstream [7]. In some cases the whole riser

will be filled with liquid until the pressure of the gas is large enough to overcome the hydrostatic pressure. With this condition given, a cyclic operation is obtained [4]. Terrain slugging is sometimes referred to as severe slugging, as these slugs can become hundreds of meters long. The hydrodynamic slugs are shorter. Riser slugging in pipeline-riser systems can be given as cyclic operations described in four steps, see figure 2.1.

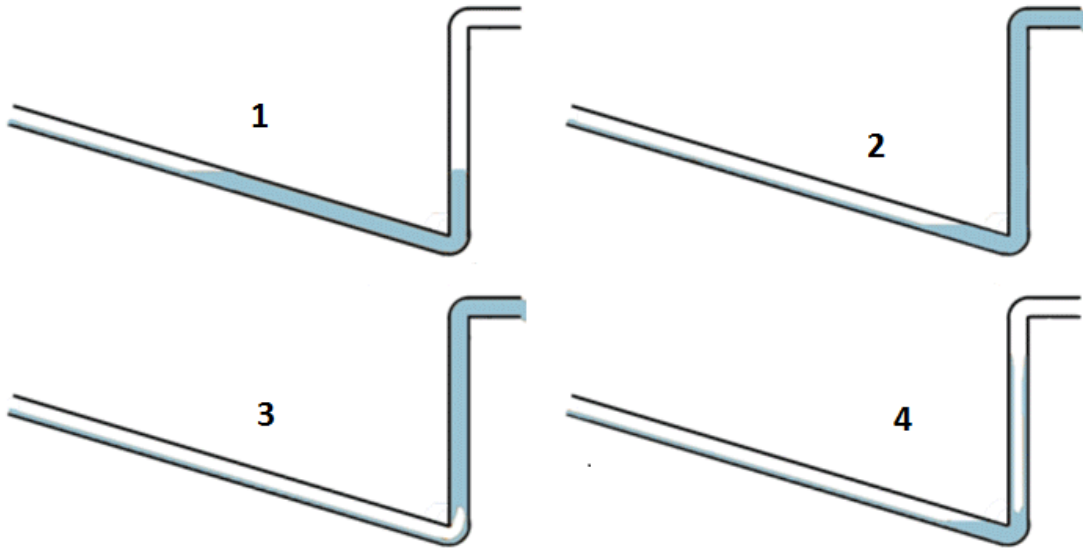


Figure 2.1: Illustration of the riser slugging in pipeline-riser systems [1]

First liquid accumulates in the low-point of the riser, blocking the gas. Gas pressure is equal at both sides of the liquid (1). More liquid and gas enter the pipeline, the pressure increase and the riser is filled with liquid. Gas pressure builds up on the upstream side (2). After some time the amount of gas that is blocked will be large enough to blow the liquid out of the riser (3). After the blow-out of liquid, a new liquid slug will start to form in the low-point and some of the liquid will fall back (4). This behavior repeats and is the reason it is called a cyclic process. [7]

Slug flow has a negative impact on equipment in offshore oil and gas production. Normal problems are flaring and reduced operating capacity. It can also lead to stress on valves and bends. Also seen are problems in the separator and the compressor trains and this can lead to damages. Worst case scenario is plant shutdown, as these unforeseen shutdowns are extremely expensive and should be avoided. [7]

There are options to avoid or manage slugging, e.g. altering the design of the process. This can be a change in the pipeline geometry, increase the size of the separator, add a slug catcher or install a gas lift. Some off-shore plants use gas lift and therefore do not transport the gas they produce. Gas lift is when gas is pumped down to the base of the riser. Slugs are avoided as this method increase pressure and gas flow at the bottom. If a gas lift is used, the composition in the flow and the flow regime are altered, but this is an expensive solution. As both gas lift and installation of new equipment is expensive, other options should be considered. Another option is changing the operating conditions by choking the topside valve [4]. A drawback when choking is used is increased pressure in the pipeline. This leads to a reduced production

rate and it can also lower the total recovery of the field that is exploited [4]. The last decade's active control has been study and this can be use as a tool to avoid the slug flow regime by stabilizing the flow. The goal with control-based solution is to stabilize a flow region which otherwise would be unstable. Active control changes the boundaries of the flow map and with this it is possible to operate with the same flow rates as before, but without oscillations in flow rates and pressures [4]. Advantages with active control implemented are large. It is much cheaper than new equipment and it removes slug flow and thereby removes strain on system. Cost used on maintenance is saved.

## 2.3 Simplified model

A simplified model was used to perform the controllability analysis, and to study different stabilizing control solutions. There are five different published simplified models for severe slug flow. It was chosen to use the new simplified model made by Esmaeil Jahanshahi [5]. This model is for an L-riser and is a dynamic low order model. This model separates the liquid mass of the system into two state variables, and this corresponds to the liquid content of the pipeline and the riser section. If the mass of the liquid in the pipeline is available then it will be possible to calculate the volume of gas. In the start of October the model was altered to a certain extent where a new tuning parameter was taken into use. Friction factor in the pipeline and riser was also included. The most significant results was that the zeros went from being complex zeros to real zeros, when  $Z > 5\%$ , for measurement  $P_2$ . The model with four tuning parameters and friction factor will be used in the analysis and control part of the project. The model will be explained shortly below, for a more thorough study see appendix B.

The new model use four tuning parameters, this makes the model more relevant to the real world. These tuning parameters are the choke valve constant ( $K_{pc}$ ), an orifice coefficient for gas flow through the low point ( $K_G$ ), a orifice coefficient for liquid flow through low point ( $K_L$ ) and the last is a correction factor for level of liquid in pipeline ( $K_h$ ). Four state variables are used and these are listed below. Each state variable have a state equation and these are given in equations 2.1, 2.2, 2.3 and 2.4.

- $m_{G1}$ : Mass of gas in the pipeline
- $m_{L1}$ : Mass of liquid in the pipeline
- $m_{G2}$ : Mass of gas in the riser
- $m_{L2}$ : Mass of liquid in the riser

$$\frac{dm_{G1}}{dt} = w_{G,in} - w_{G,lp} \quad (2.1)$$

$$\frac{dm_{L1}}{dt} = w_{L,in} - w_{L,lp} \quad (2.2)$$

$$\frac{dm_{G2}}{dt} = w_{G,lp} - w_{G,out} \quad (2.3)$$

$$\frac{dm_{L2}}{dt} = w_{L,lp} - w_{L,out} \quad (2.4)$$

The chosen model was linearized in MATLAB (see chapter 4.1), and this linear model has one input  $u$  ( $Z$ =choke valve opening), two disturbances ( $w_{G,in}$  and  $w_{L,in}$ ) and four outputs ( $P_1$ ,  $P_2$ ,  $W$  and  $Q$ ). The model has actually three outputs, but with small changes in the linearization of the model it can be changed between  $Q$  and  $W$  as third output.  $P_1$  is the inlet pressure,  $P_2$  is the outlet pressure also called the topside pressure,  $W$  is the mass flow rate from the choke valve and  $Q$  is the volumetric flow rate from the choke valve. The model used has a inlet flow of 9kg/s.

OLGA has been used as a reference to tune the model, as this is a simulation close to the real situation. As this is a simulation it will deviate from a real riser slugging, e.g. OLGA has a volume error. The simple model was compared to the OLGA reference model in the following five aspects listed below, in order of importance.

1. Stability margin (the critical valve opening).
2. Frequency of the oscillations in the critical point.
3. Response to the step change in the valve opening.
4. Prediction of the steady state value.
5. Maximum and minimum of the oscillations.

### 3 Simulation in OLGA and bifurcation diagrams

To study the dynamic behavior of the slugging in an L-riser a simulator, OLGA, was used. OLGA is made by the SPT group and is the leading simulator for flow of oil, water and gas. The L-riser model in OLGA was pre-existent. To get a good design for a multiphase production system an understanding of flow behavior is important. OLGA will provide solution through accurate modelling of true dynamics [9]. Simulations were performed to get a better understanding of what happens in a riser, and also to get to know OLGA as a simulator. Bifurcation diagrams were made for two different inlet flows, 9 kg/s and 12 kg/s, to determine where slugging starts in open loop (the bifurcation point). A picture of the riser model in OLGA is given in figure 3.1. In the OLGA model, the pipeline diameter is 0,12 m, and the length is 4300 m when starting from inlet. This length consists of a 2000 m long horizontal pipeline and the remaining 2300 m is inclined with  $1^\circ$ . This causes a 40,14 m decent and creates a low point at the end of the pipeline. The riser is a vertical pipeline on 300 m, with a diameter of 0,1 m. As a finish there is a 100 meter horizontal pipeline that connects the riser to the outlet choke valve. The feed into the system is nominally constant at 9 kg/s and 12 kg/s.



Figure 3.1: Illustration of the riser model with geometry

#### 3.1 Bifurcation diagrams

Bifurcation diagrams were made by simulation in OLGA for different choke openings, and the bifurcation diagram for the new simple model was found by using MATLAB. To plot the bifurcation diagram of the new simple model, a MATLAB file made by Esmail Jahanshahi was used. A bifurcation point is where slugging starts in open loop. This point is a specific parameter value where the qualitative behavior of a nonlinear differential equation system changes significantly. The bifurcation diagram given here, show the behavior of the system over the working range, choke valve opening 0-100 % ( $Z$ ). First the bifurcation diagram for a constant inlet feed at 9 kg/s is given in figure 3.2a. The dashed and solid line in the middle of the plots gives desired non-oscillatory flow regime, which is unstable without control. OLGA includes a steady-state preprocessor which is intended for calculating initial values to the transient simulations [5]. For unstable operating point, initial values provided by OLGA are considered as steady state values. For  $Z > 5\%$  in

addition to the steady state solution, there are two other lines given the maximum and minimum pressure and flow rates of the oscillations. The OLGA model has red dash lines and new model have black solid lines. For 12 kg/s as inlet feed, a bifurcation diagram is given in figure 3.2b. The OLGA model has black solid lines and the new model has red dashed lines. The lines in the middle is the same as if was for 9 kg/s. For  $Z > 12\%$ , there are two other lines given, and this is the maximum and minimum pressures and flow rates of the oscillations.

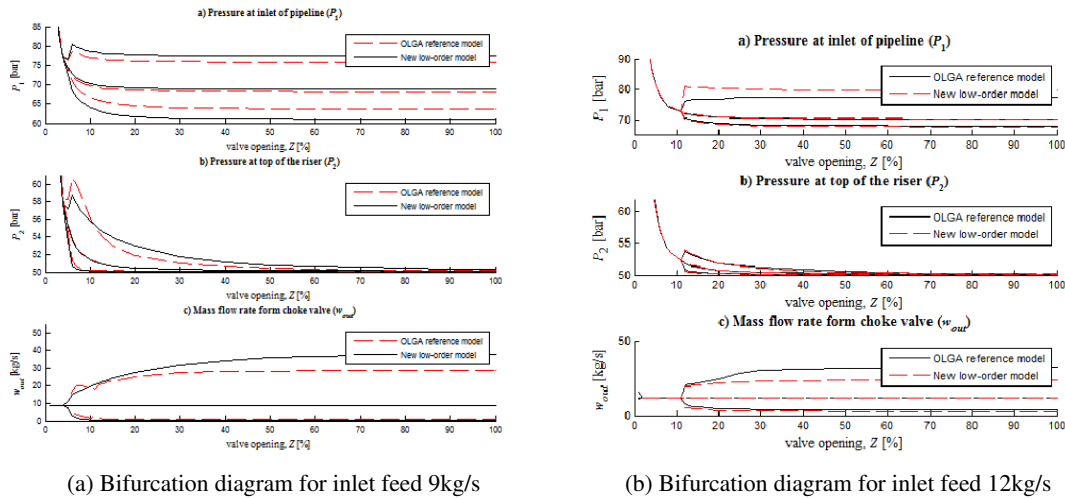


Figure 3.2: Bifurcation diagrams

It can be confusing and not understandable when maximum and minimum pressure and flow rate of the oscillations is used in the explanation. To make bifurcation diagrams, simulations with different choke openings were done. Some chosen variables ( $W$ ,  $P_1$ ,  $P_2$  and  $Q$ ) were decided to use and all these simulated values was imported to excel. By taking the maximum-, minimum- and steady state values from all these simulated values at each choke valve opening, a bifurcation diagram could be made. For  $Z < 5\%$  there was no oscillations because of stable flow, but for  $Z > 5\%$  oscillation will occur as the flow is unstable. Riser slugging is easily observed. To give a picture of this, figure 3.3a and 3.3b is showing the simulated mass flow rate out for  $Z=10\%$  (unstable) and  $Z=3\%$  (stable). These figures are for an inlet flow 9kg/s.

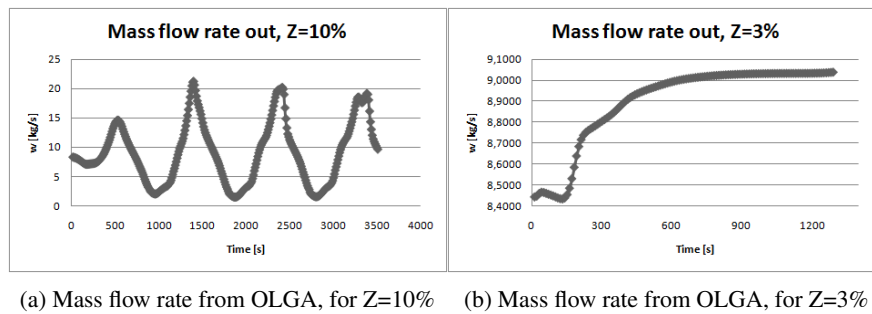


Figure 3.3: Simulation results from OLGA

The simulation in OLGA was done as this gave a better understanding of the riser slugging phenomena. OLGA was learned and a course in OLGA was performed in the project time. A smart thing in OLGA that should be mentioned is to use the "run batch" procedure instead of the play button. The simulation will then proceed faster. For 9kg/s the bifurcation point is  $Z \approx 5\%$ , and for 12 kg/s it is  $Z \approx 12\%$ . The bifurcation point for 12kg/s is greater than the one for 9kg/s as more inlet flow is used in the riser. This increase the power to push the liquid through the riser. As a result severe slugging is avoided when  $Z < 12\%$ .

## 4 Controllability analysis of two-phase pipeline-riser system

To control the riser slugging we need some analysis, because riser slugging is a challenging task to control. Subsea measurements e.g. inlet pressure have proved to effectively stabilize the flow [4]. If no subsea measurements are available the task gets far more challenging. As subsea measurements are more costly to implement and maintain, an interest in topside measurements have increased. A closer study of topside measurements have been performed to see if it is possible to stabilize the flow with control, using only measurements from topside of the riser system.

A controllability analysis is able to find measurement candidates most suited for stabilizing control by using a linear model, and in this project a dynamic model made by Esmail Jahanshahi was used. A scaled linear model was used to perform the evaluation of the different measurements. Four different measurements were evaluated and minimum peaks on different closed-loop transfer functions were found. The measurements evaluated are; inlet pressure ( $P_1$ ), topside pressure ( $P_2$ ), volumetric flow rate ( $Q$ ) and mass flow rate ( $W$ ). Measurements are the measured outputs available in this model. Pressure measurements are often reliable measurements for stabilizing control, but the location of the pressure sensors may have a significant impact on the controllability of the system. The measurements were evaluated separately in analysis, so a SISO system was considered with one measurement, and this can be used in a single-loop control system. Control based on two measurements e.g.  $P_2$  and  $Q$  are used in section 6, and controllability analysis was performed on this SIMO control system for some of the bounds.

### 4.1 Linearization

The nonlinear model had to be linearized, and this was performed in MATLAB. Linearization was completed with three methods; analytical, numerical and by using the "linmod" functions in MATLAB. These three methods gave an equal state space model (A, B, C and D matrices), so for further work analytical linearization was used. Linearization was done around an operating point (choke valve opening  $Z$ ), and this can be altered to give both stable and unstable linear models. The model is stable for  $Z < 5\%$  and unstable for  $Z > 5\%$ , found by the bifurcation diagram. This could also be found by looking at the poles for the linear models linearized around different operating points. The linear model had RHP-poles when  $Z > 5\%$ . Two different cases were first considered to be used in the analysis, which also resulted in two different linear models. The first case was with  $\bar{\alpha}_{L1}$  constant and the second case with  $\bar{\alpha}_{L1}$  not constant, when linearization was performed. Both cases were actually used until one week before deadline of the project. Simulations with step-changes in both linear, nonlinear and OLGA model were performed and compared. It was found that  $\bar{\alpha}_{L1}$  should have been kept constant in the linearization, as this is the most realistic case and close to the reference model in OLGA. For the simple model used in this project, it is not correct to use  $\bar{\alpha}_{L1}$  not constant. It was therefore decided to only use the correct result with keeping  $\bar{\alpha}_{L1}$  constant when linearization was performed. A linearization was performed, which obtained A, B, C and D matrices given below in equation 4.1, when  $Z=10\%$ .

$$\begin{aligned}
A &= \begin{bmatrix} -0,0144 & 0,0570 & 0,2144 & 0,0143 \\ -0,3385 & -0,5221 & 5,1165 & 0,3403 \\ 0,0144 & -0,1051 & -0,3607 & -0,0218 \\ 0,3385 & 0,8683 & -8,4594 & -0,5380 \end{bmatrix} \\
B &= \begin{bmatrix} 0 & 1,2086 & -0,0562 \\ 0 & 4,9793 & 2,3420 \\ -3,6000 & -0,2086 & -0,0562 \\ -86,400 & -4,9793 & -1,3420 \end{bmatrix} \\
C &= \begin{bmatrix} 0,0666 & 0,0046 & 0 & 0 \\ 0 & 0 & 1,0036 & 0,0575 \\ 0 & -0,2980 & 3,4892 & 0,2052 \end{bmatrix} \\
D &= \begin{bmatrix} 0 & 0 & 0 \\ 0 & 0 & 0 \\ 90 & 0 & 0 \end{bmatrix}
\end{aligned} \tag{4.1}$$

The system has complex RHP-poles for  $Z > 5\%$ , but for  $Z > 20\%$  RHP-poles are real. The only measurement of the ones considered in this project which introduces RHP-zeros into the system, is the topside pressure. The topside mass flow rate has a zero ( $z$ ) that is very close to the origin, so it is set to be zero in the controllability analysis. This was done because this zero is  $-1e-14$  for some choke openings, and  $1e-14$  for other operating points when linearization is performed. This has to do with the accuracy that MATLAB have in calculations.

As mentioned, the topside pressure measurement has RHP-zeros, and the RHP-poles and RHP-zeros are getting closer to each other when the choke valve opening increase. As this is an important task in this project, these poles and zeros are given in table 4.1. RHP-poles and RHP-zeros give limitations when  $P_2$  is used for stabilizing control, and they give significant problems when they are getting closer to each other. The limitation on achievable control performance will be explained in section 6.2.

## 4.2 Scaling the system

Before the controllability analysis could be performed, the models were scaled as outlined in Skogestad and Postlethwaite 2005 [3]. This was performed so all signals in the system are less than one in magnitude. This is both to include saturation effect and to be able to compare signals of different magnitude. Scaled variables and models make the model analysis and controller design simpler. To do the scaling, decisions were made on expected magnitudes of disturbances, reference change, and allowed magnitude of each input signal. For MIMO systems, each variable that are scaled may have a different maximum or allowed value. Three diagonal scaling matrices  $D_u$ ,  $D_d$  and  $D_e$  are used. This introduces two scaled transfer-function matrices  $G$  and  $G_d$ , given in equation 4.2 and 4.3.

$$G = D_e^{-1} G D_u \tag{4.2}$$

$$G_d = D_e^{-1} G_d D_d \tag{4.3}$$

Table 4.1: Topside pressure: Zeros and Poles

Choke valve opening (Z) [%]	Pole 1	Pole 2	RHP-zero 1	RHP-zero 2
4	-0,0008 + 0,0056i	-0,0008 - 0,0056i	0,0360	0,0150
5	0,0000 + 0,0067i	0,0000 - 0,0067i	0,0413	0,0126
7	0,0021 + 0,0085i	0,0021 - 0,0085i	0,0455	0,0111
10	0,0057 + 0,0099i	0,0057 - 0,0099i	0,0476	0,0104
15	0,0116 + 0,0091i	0,0116 - 0,0091i	0,0487	0,0101
20	0,0162 + 0,0050i	0,0162 - 0,0050i	0,0491	0,0100
25	0,0261	0,0128	0,0493	0,0099
30	0,0321	0,0115	0,0494	0,0099
40	0,0388	0,0107	0,0495	0,0099
50	0,0424	0,0103	0,0495	0,0099
70	0,0457	0,0101	0,0496	0,0099
90	0,0472	0,0100	0,0496	0,0099

Outputs were scaled with the maximum allowed deviation, given in the diagonal matrix  $D_e$ . In this scaling both  $Q$  and  $W$  are scaled with the same maximum allowed deviation (1 L/s and 1 kg/s). The matrix shows only three outputs, as this is used in the model ( $P_1$ ,  $P_2$  and  $Q$  or  $W$ ). As mentioned, small changes in linearization can be performed to change between  $Q$  and  $W$  as output. The inlet- and topside pressures have been scaled with an allowed deviation of 1 bar. The input was scaled with the minimum allowed positive deviation in valve opening, given in  $D_u$ . For example, with a valve opening of  $Z = 30\%$ , the input scaling is  $D_u=30\%$ . If the valve opening is  $Z = 60\%$ , then the input scaling is  $D_u=40\%$ . Flow variations into the pipeline are represented as disturbances and scaled by using allowed deviation in the feed, determined to be 10%, in discussion with the supervisors. The three scaling matrices are given in 4.4, 4.5 and 4.6.

$$D_u = \min(z0, 1 - z0) \quad (4.4)$$

$$D_e = \begin{bmatrix} 1 & 0 & 0 \\ 0 & 1 & 0 \\ 0 & 0 & 1 \end{bmatrix} \quad (4.5)$$

$$D_d = \begin{bmatrix} 0,04 & 0 \\ 0 & 1 \end{bmatrix} \quad (4.6)$$

### 4.3 Controllability analysis: Theoretical background

The controllability analysis used in this project is from Skogestad and Postlethwaite (2005) [3] and Chen (2000) [10].

Input-output controllability is the ability to achieve acceptable control performance in a plant, with any controller. Before the controller system is designed one should determine how readily the plant is to control. Decisions have to be made about which variables that should be used to measure and control, and which variables should be manipulated. A definition is given in Skogestad and Postlethwaite (2005) for input-output controllability.

**Definition 1.** *(Input-output) controllability is the ability to achieve acceptable control performance; that is, to keep the output ( $y$ ) within specified bounds or displacements from their references ( $r$ ), in spite of unknown but bounded variations, such as disturbances ( $d$ ) and plant changes, using available inputs ( $u$ ) and available measurements.*

This definition should not be confused with the concept of "state controllability" given by Kalman in the 1960's. State controllability is the ability of an external input to move the internal state of a system, from any initial state to any other final state in a finite time interval. State controllability is important for numerical calculations and realization [11].

To summarize the main point in input-output controllability; For a plant to be controllable there have to exist a controller that yields acceptable performance for all expected variations. Controllability is a property of the plant and is independent of the controller. Controllability analysis performed is a simple method that can be used to get an idea of how readily the plant is to control, and which measurements that are able to stabilize the process with a controller. This simple method is based on appropriately scaled models of  $G(s)$  and  $G_d(s)$ . Controllability analysis is performed on linear models.

To understand the controllability analysis consider the process  $y = G(s)u + G_d(s)d$ , with input to the process given as  $u = K(s)(r - y - n)$  when the process is controlled with a controller  $K(s)$ . Closed loop response is then given as  $y = Tr + SG_d d - Tn$ . In this closed loop response  $S$  is sensitivity function, and  $T$  is complementary sensitivity function given in equation 4.7 and 4.8, where  $T+S=I$ .

$$S = (I + GK)^{-1} \quad (4.7)$$

$$T = (I + GK)^{-1} GK \quad (4.8)$$

Control error is  $e = y - r = -Sr + SG_d d - Tn$  and this give plant input to be  $u = KSr - KSG_d d - KSn$ . The results given are different closed-loop transfer functions that are used in controllability analysis, independent of the controller  $K$ . By obtaining the lower bounds on the closed-loop transfer functions  $S$ ,  $T$ ,  $KS$ ,  $SG$ ,  $KSG_d$  and  $SG_d$ , information about achievable performance and possible robustness problems will be found. The bounds considered are on the  $H_\infty$  norm,  $\|M\|_\infty = \max_{\omega} |M(j\omega)|$ , and this gives the peak value for the different transfer functions. By this the "peak" is the maximum value of the frequency response of  $M$ .

In Skogestad and Postlethwaite (2005), there are two chapters about minimum peaks for closed-loop transfer functions. Some fundamental algebraic and analytic constraints for the different closed-loop transfer functions will be given. SISO systems are considered in chapter 5, and these bounds are "tight" for one RHP-pole and one RHP-zero. A tight bound indicates that there exists a controller (possibly improper) that achieves the bound, and with equality. For example, with a single RHP-zero and no time delay,  $\min_K \|S\|_\infty = M_{S,\min} =$

$M_{zpi}$ . There are measurements with multiple RHP- poles and RHP-zeros in the model used for the riser-slugging system, and bounds in chapter 5 will not be tight for this system. In chapter 6 minimum peaks for different transfer functions in a MIMO system are considered. Almost all these bounds are tight for multiple RHP- poles and zeros. The controllability analysis has been divided into two parts for analysis of the riser slugging system. The first is called method 1 and is based on bounds given in chapter 5. The second is called method 2 and based on bounds given in chapter 6, where some of the bounds are tight for riser slugging system.

### 4.3.1 Minimum peaks on $S$ and $T$

The closed-loop transfer function  $S$  is from output disturbances to the outputs, and  $T$  is the closed-loop transfer function from reference signals to the outputs. The lowest achievable peaks in  $S$  and  $T$  are closely related to the distance between the unstable poles and zeros. The minimum achievable peaks in  $S$  and  $T$  are given as  $M_{S,min}$  and  $M_{T,min}$ . This denote lowest achievable values for  $\|S\|_\infty$  and  $\|T\|_\infty$ , by using any stabilizing controller  $K$  and is defined as given in equations 4.9 and 4.10.

$$M_{S,min} \triangleq \min_K \|S\|_\infty \quad (4.9)$$

$$M_{T,min} \triangleq \min_K \|T\|_\infty \quad (4.10)$$

For a plant with a single RHP-zero and any number of RHP-poles equation 4.11 gives a tight lower bound on  $\|S\|_\infty$  and  $\|T\|_\infty$ . For a plant with a single RHP-pole and any number of RHP-zeros equation 4.12 gives a tight lower bound on  $\|S\|_\infty$  and  $\|T\|_\infty$ . Both these lower bounds were calculated, and the bound that gave the highest value are used in the results given later.

$$M_{S,min} = M_{T,min} = \prod_{i=1}^{N_p} \frac{|z + p_i|}{|z - p_i|} = M_{zpi} \quad (4.11)$$

$$M_{S,min} = M_{T,min} = \prod_{j=1}^{N_z} \frac{|z_j + p|}{|z_j - p|} = M_{pzj} \quad (4.12)$$

For method 2, the bound is given for any number of RHP-poles and RHP-zeros. If the plant  $G(s)$  is without time delay (rational) and there is  $N_z$  RHP-zeros ( $z_i$ ) and  $N_p$  RHP-poles ( $p_i$ ) with output zero and pole direction, then the following tight lower bound on  $\|S\|_\infty$  and  $\|T\|_\infty$  are given in equation 4.13.

$$M_{S,min} = M_{T,min} = \sqrt{1 + \bar{\sigma}^2(Q_z^{-1/2} Q_{zp} Q_p^{-1/2})} \quad (4.13)$$

In equation 4.13  $Q_z$  is  $N_z \times N_z$ ,  $Q_p$  is  $N_p \times N_p$  and  $Q_{zp}$  is  $N_z \times N_p$ . How to find  $Q_z$ ,  $Q_p$  and  $Q_{zp}$  is given in equation 4.14. In this equation  $y_{z,i}$  is the output zero direction vector and  $y_{p,i}$  is the output pole direction vector.

$$[Q_z]_{ij} = \frac{y_{z,i}^H y_{z,j}}{z_i + \bar{z}_j}, [Q_p]_{ij} = \frac{y_{p,i}^H y_{p,j}}{\bar{p}_i + p_j}, [Q_{zp}]_{ij} = \frac{y_{z,i}^H y_{p,j}}{z_i + p_j} \quad (4.14)$$

Large values for  $\|S\|_\infty$  and  $\|T\|_\infty$  imply poor performance and robustness problems. Time delays pose limitations, and the bound for  $\|T\|_\infty$  is increased by a factor  $|e^{p\theta}|$  for a single RHP-pole and by at least a factor  $|e^{p_i\theta}|$  for multiple poles.

### 4.3.2 Minimum peaks on $KS$

The peak on the transfer function  $KS$  has to be as small as possible, as it is important to avoid large input signals in response to noise and disturbances. This is particular important for unstable systems, that happens in the riser system when  $Z > 5\%$ . A large value of  $\|KS\|_\infty$  will most likely cause saturation in input and this will further result in difficulties in stabilizing the system.

A simple bound is possible to use, as for any RHP-pole,  $\underline{\sigma}_H(\nu(G)^*) \leq |G_s(p)|$  and  $G_s(s)$  is the stable version of  $G$ . A stable version of  $G$  is the RHP-poles mirrored into the LHP. This bound is given in equation 4.15, and equality applies for a plant with a single real RHP-pole. This bound is only tight for plants with a single real RHP-pole, and this bound was used in method 1.

$$\|KS\|_\infty \geq |G_s^{-1}(p)| \quad (4.15)$$

The bound used in method 2 is given in equation 4.16. In this bound the smallest Hankel singular value ( $\underline{\sigma}_H$ ) of the mirror image of the anti-stable part of  $G$  is used. The bound in equation 4.16 is tight for multiple and complex RHP-poles, and there always exists a controller (possibly improper) that achieves the bound. If the plant is stable there exists no lower bound, as  $\min_K \|KS\|_\infty = 0$  and that is achieved by  $K=0$ .

$$\|KS\|_\infty \geq 1/\underline{\sigma}_H(\nu(G)^*) \quad (4.16)$$

### 4.3.3 Minimum peaks on $KSG_d$

The bound 4.15 can be generalized to get a new bound given in equation 4.17, for  $KSG_d$ . This is only tight for a single RHP-pole, and therefore used in method 1. In equation 4.17  $G_{d,ms}$  denotes the stable and minimum-phase version of  $G_d$ , with both the RHP-poles and RHP-zeros mirrored into the LHP.

$$\|KSG_d\|_\infty \geq |G_s^{-1}(p)G_{d,ms}(p)| \quad (4.17)$$

For disturbances the bound in equation 4.16 can be generalized as given in equation 4.18. In this equation the minimum of the Hankel singular value of the mirror image of the anti-stable part of  $G_{d,ms}^{-1}G$  is used. This bound was used in method 2, as this is tight for multiple and complex RHP-poles [2].

$$\|KSG_d\|_\infty \geq 1/\underline{\sigma}_H(\nu(G_{d,ms}^{-1}G)^*) \quad (4.18)$$

#### 4.3.4 Minimum peaks on $SG$

Transfer function  $SG$  should be small to reduce the effect input disturbance have on the control error signal. This transfer function should also be small for robustness against pole uncertainty. Uncertainties have not been considered in this project. Because of the interpolation constraints, a controller that stabilize  $S$  will also stabilize  $SG$ . Further,  $\|SG\|_\infty = \|SG_{ms}\|_\infty$ , where  $G_{ms}$  is the "minimum-phase, stable version" of  $G$ . The "minimum-phase, stable version" of  $G$  is given in equation 4.19.

$$G_{ms} \triangleq \prod_i \frac{s-p_i}{s+p_i} \cdot G(s) \cdot \prod_j \frac{s-z_j}{s+z_j} \quad (4.19)$$

The bound for  $\|SG\|_\infty$  is given in equation 4.20, and is tight for plants with a single RHP-zero.  $G_m$  is the "minimum-phase" version of  $G$ . The bound for  $SG$  is valid for any RHP-zero so the bound can be applied for systems with multiple unstable zeros. This bound was used in method 1.

$$\|SG\|_\infty \geq |G_{ms}(z)| \cdot \prod_{i=1}^{N_p} \frac{|z+p_i|}{|z-p_i|} = |G_m(z)| \quad (4.20)$$

For a system with one RHP-zero and one RHP-pole,  $\|SG\|_\infty$  must satisfy the bound given in equation 4.21. In Skogestad and Postlethwaite (2005) it was not written which norm that was used in 4.21, for the first term on the right side. It was concluded that it was norm two, from Chen (2000) [10].  $G_{ms}(s)$  should also be replaced by  $G_{ms}(z)$ , and the new correct equation for this bound is given in equation 4.22. As topside pressure has multiple RHP-pole and RHP-zero in the riser slugging system, it was chosen one zero and pole to be used for calculation. The chosen pole and zero, was the two that gave the highest peak value. This bound given in equation 4.22 and this was used in method 2, but it is only tight for systems with one RHP-zero and one RHP-pole.

$$\|SG\|_\infty \geq \|y_z^H G_{ms}(s)\| \sqrt{\sin^2 \tilde{\phi} + \frac{|z+\bar{p}|^2}{|z-p|^2} \cos^2 \tilde{\phi}} \quad (4.21)$$

$$\|SG\|_\infty \geq \|y_z^H G_{ms}(z)\|_2 \sqrt{\sin^2 \phi + \frac{|z+\bar{p}|}{|z-p|} \cos^2 \phi} \quad (4.22)$$

where

$$\cos \tilde{\phi} = \frac{|y_z^H G_{ms}(z) G_{ms}^{-1}(p) y_p|}{\|y_z^H G_{ms}(z)\|_2 \|G_{ms}^{-1}(p) y_p\|_2} \quad (4.23)$$

#### 4.3.5 Minimum peaks on $SG_d$

The bound on  $SG_d$  is given in 4.24, and this should be kept small. The reason for keeping this bound small is to reduce the effect of disturbances on the outputs. This bound can be handled similar to  $SG$  by replacing  $G_{ms}$  with  $G_{d,ms}$ . The bound for  $SG_d$  is only tight for one RHP-zero, but it is valid for any RHP-zero so the

bound can be applied for systems with multiple unstable zeros. This bound was used in method 1.

$$\|SG_d\|_\infty \geq |G_{d,ms}(z)| \cdot \prod_{i=1}^{N_p} \frac{|z + p_i|}{|z - p_i|} \quad (4.24)$$

For method 2, the bound given in equation 4.25 was used. This bound is tight for a system with one RHP-zero and one RHP-pole, and the pole and zero that gave the highest peak for this bound was used in the results.

$$\|SG_d\|_\infty \geq \|y_z^H G_{d,ms}(z)\|_2 \sqrt{\sin^2 \tilde{\phi} + \frac{|z + \bar{p}|^2}{|z - p|^2} \cos^2 \tilde{\phi}} \quad (4.25)$$

where

$$\cos \tilde{\phi} = \frac{|y_z^H G_{d,ms}(z) G_{d,ms}^{-1}(p) y_p|}{\|y_z^H G_{d,ms}(z)\|_2 \|G_{d,ms}^{-1}(p) y_p\|_2} \quad (4.26)$$

#### 4.3.6 Comment

Time delay was not considered in the linear models. Time delays could have been found and used as RHP-zeros in the controllability analysis. In a real process there is always time delay independent of which controller used. For choke valve openings that give complex RHP-poles, method 1 and 2 are not readily to compare. For  $Z \geq 25\%$ , both the RHP-poles and RHP-zeros are real, and the two different methods are more comparable.

MATLAB was used to perform the controllability analysis and these files are given in appendix E for both methods. A function named *stabsep* in MATLAB was used. This function decomposes the LTI model  $G$  into its stable and unstable parts,  $G = GS + GNS$ .  $GS$  contains all stable modes that can be separated from the unstable modes in a numerically stable way, and  $GNS$  contains the remaining modes.  $GNS$  is always strictly proper and in some cases the function takes zeros close to the origin and count them as a part of the unstable part, even if it is zero negative. This can be handled by using *stabsepOptions*. For further explanation use the product help in MATLAB.

In previous controllability analysis it was observed that only real values of the RHP-pole and RHP-zero was used in the calculations of minimum peak values, when RHP-poles and RHP-zeros were complex. This is not correct, and as MATLAB can calculate with complex number these should be used.

## 4.4 Results and discussion of controllability analysis

In controllability analysis a simple model have been used, and four alternative measurements have been evaluated. These are the inlet pressure ( $P_1$ ), topside pressure ( $P_2$ ), mass flow rate topside ( $W$ ) and volumetric flow rate topside ( $Q$ ). As measurements have been evaluated separately this is actually a SISO controllability analysis.

Topside pressure as measurement introduce RHP-zeros independent of the choke valve opening, and both poles and zeros were given in table 4.1. An unstable system has RHP-poles, and this occur when choke valve opening is larger than the critical for the process. Critical choke opening is  $\approx 5\%$ , and a larger choke opening will give riser slugging. Controllability analysis results are given for three operating points Z (choke valve opening). The first opening is 3% and the system is stable. The second opening is 10%, where instability is slow. The last choke opening is 30%, where instability is fast and a stable system is more difficult to achieve. Stationary gain and the minimum peaks on different closed-loop transfer functions will be given. Stationary gain for each measurements are given for several other choke valve opening in appendix C. The bounds in method 1 and three bounds in method 2 are not tight for this system, as the different measurements and overall system have several RHP-zeros and RHP-poles. The bound on  $SG$ ,  $SG_{d1}$  and  $SG_{d2}$  in method 2 are not tight for this system. To find the minimum peak on these transfer-functions one pole and one zero were chosen to be used. As this system is scaled, all signals in the system should be less than one in magnitude. Measurements that have peak values smaller than one for all closed-loop transfer functions, are most suited for stabilizing control.

A Kalman filter based on two measurements,  $P_2$  and  $Q$ , is used in section 6. This can be considered as a SIMO control system and a controllability analysis for this system was performed. This is called a SIMO system because the inlet disturbances are not considered as inputs, but of course they could be and this had then been named a MIMO system. The bound on  $S$  and  $KS$  were chosen to be considered for this system. Equation 4.13 and 4.16 were used (method 2). All bounds should have been considered, but because of limited time it was chosen to only consider the bounds on  $S$  and  $KS$ .

#### 4.4.1 Minimum peaks for different closed-loop transfer functions

Results for method 1 for three different choke valve openings are given in table 4.2.

Table 4.2: Results from method 1

Measurement	$G(0)$	$ S = T $	$ KS $	$ KSG_{d1} $	$ KSG_{d2} $	$ SG $	$ SG_{d1} $	$ SG_{d2} $
$P_1$ (Z=3%)	26,0570	1	0	0	0	0	0	0
$P_1$ (Z=10%)	2,7561	1	0,4144	0,0789	0,3391	0	0	0
$P_1$ (Z=30%)	0,3126	1	6,3053	0,5998	2,3474	0	0	0
$P_2$ (Z=3%)	24,5945	1	0	0	0	0	0	0
$P_2$ (Z=10%)	2,5641	3,0022	0,8279	0,0931	0,4483	6,8119	0,2716	1,3145
$P_2$ (Z=30%)	0,2903	25,0555	74,8429	0,8539	4,2125	7,1738	0,2815	1,7764
$Q$ (Z=3%)	2,3788	1	0	0	0	0	0	0
$Q$ (Z=10%)	0,3768	1	0,1186	0,0930	0,4151	0	0	0
$Q$ (Z=30%)	0,0446	1	1,1507	0,8537	3,5513	0	0	0
$W$ (Z=3%)	6,6917E-14	1	0	0	0	0	0	0
$W$ (Z=10%)	6,3830E-15	1	0,2268	0,0931	0,4849	0	0	0
$W$ (Z=30%)	5,3076E-16	1	2,5290	0,8540	5,0332	0	0	0

Results from method 2 for three different choke valve openings, are given in table 4.3.

Table 4.3: Results from method 2

Measurement	G(0)	$ S = T $	$ KS $	$ KSG_{d1} $	$ KSG_{d2} $	$ SG $	$ SG_{d1} $	$ SG_{d2} $
P <sub>1</sub> (Z=3%)	26,0570	1	0	0	0	0	0	0
P <sub>1</sub> (Z=10%)	2,7561	1	0,5501	0,1439	0,3841	0	0	0
P <sub>1</sub> (Z=30%)	0,3126	1	7,7573	1,2690	2,6691	0	0	0
P <sub>2</sub> (Z=3%)	24,5945	1	0	0	0	0	0	0
P <sub>2</sub> (Z=10%)	2,5641	3,5486	1,2109	0,1440	0,6529	4,5392	0,1810	0,8760
P <sub>2</sub> (Z=30%)	0,2903	32,1361	110,3915	1,2505	5,7588	3,8044	0,1493	0,7193
Q (Z=3%)	2,3788	1	0	0	0	0	0	0
Q (Z=10%)	0,3768	1	0,1554	0,1440	0,5581	0	0	0
Q (Z=30%)	0,0446	1	1,5828	1,2506	4,6177	0	0	0
W (Z=3%)	6,6917E-14	1	0	0	0	0	0	0
W (Z=10%)	6,383E-15	1	0,3602	0,1441	0,7524	0	0	0
W (Z=30%)	5,3076E-16	1	3,9417	1,2506	7,2247	0	0	0
Q and P <sub>2</sub> (Z=10%)	-	1,0399	0,15404	-	-	-	-	-
Q and P <sub>2</sub> (Z=30%)	-	1,7498	1,5827	-	-	-	-	-

#### 4.4.2 Discussion: Controllability analysis

Values for tight bounds are higher than values for the bounds that are not tight, and this is logical.

Topside pressure should not be used for stabilizing control because of high peaks for all bounds, and specially in the sensitivity functions,  $S$  and  $SG$ . The sensitivity peaks are larger than one for  $Z > 5\%$ . High peaks for these transfer functions are caused by RHP-zeros and RHP-poles. Lowest achievable peaks for the closed-loop transfer functions increase when the RHP-poles and RHP-zeros get closer to each other. Larger choke valve openings give closer RHP-poles and RHP-zeros, and with a large choke valve opening it becomes impossible to use topside pressure as measurement to stabilize the flow. The three other measurements,  $P_1$ ,  $W$  and  $Q$ , have peaks equal to one for the sensitivity function. These do not have RHP-zeros, and they are most suited to be used for stabilizing control. Evaluating  $|SG|$  and  $|SG_d|$  for the different operating points in method 2, one pole and one zero was chosen to be used. The pole and zero closest to each other gave the highest peak value, for both  $|SG|$  and  $|SG_d|$ . This is as expected, as close RHP-poles and RHP-zeros make the system impossible to stabilize.

Inlet pressure is most suited for stabilizing control, with a large steady state gain and smallest peak values for all closed-loop transfer functions. As this is a measurement that is not always available, it is not readily to use it for control. Mass flow rate can be used for stabilizing control from results given in analysis, but this measurement has a close-to zero stationary gain. This gives that steady-state performance is not possible, and the system will drift if this measurement is used in a single-loop controller. Evaluation of the volumetric flow rate give almost the same results as for  $W$ . Steady state gain is larger for  $Q$  than for  $W$ , but still this gain is smaller than the steady state gain for  $P_1$  and  $P_2$ , and this results in poor low-frequency performance. Both  $Q$  and  $W$  should be used as secondary measurements in a cascade controller, with  $P_1$  as primary measurement used in an outer loop. The outer loop in a cascade will take care of the low-frequency performance in the system, and the flow measurement can be used only for stabilization. These two flow measurements are suited to be used for stabilization as the peak values are low for closed-loop transfer functions considered in analysis.

Evaluation of bounds on peaks of the closed-loop transfer functions  $KS$  and  $KSG_{d(1-2)}$  for different choke valve openings, show that the peak values increase for all measurement candidates, when  $Z$  increase. Increasing the choke valve opening increases the effect disturbances and noise have on the input usage. It should in theory be possible to stabilize the system with  $P_1$ ,  $W$  and  $Q$ , when the input magnitude given by  $\|KS\|_\infty$  and  $\|KSG_{d(1-2)}\|_\infty$  are less than one. This is only for  $Z < 20\%$ , as  $\|KS\|_\infty$  exceed one for  $P_1$  and  $W$  when  $Z > 20\%$ . As the input magnitude given by  $\|KS\|_\infty$  is less than one for  $Q$  when  $Z \approx 30\%$ , volumetric flow rate should be used as measurement instead of  $W$ . The input magnitude given by  $\|KS\|_\infty$  for topside pressure as measurement is greater than one. A significant increase in the peak value occur when  $Z > 10\%$ , and when  $Z=30\%$   $\|KS\|_\infty \geq 1/\underline{\sigma}_H(v(G)^*)=110,3915$ . This gain is large, so the presence of noise or disturbance is likely to saturate the input.

A system with a combination of  $P_2$  and  $Q$  can in theory be used for stabilizing control, because the peak value barely exceed one for  $|S|$ . This result is strengthened by the input magnitude given by  $\|KS\|_\infty$ , that also is barely over one. The peak values do not increase much, even though the choke valve opening increase and this is desired when using these two measurements in combination for stabilizing control.

### 4.4.3 Controllability analysis of inlet pressure control

The inlet pressure measurements are most suited for stabilizing control, and this was confirmed in controllability analysis. In figure 4.1a the Bode magnitude plot of the linear scaled process model  $G(s)$  is given (input  $Z$  to output  $P_2$ ). This plot is obtained at the operating point  $Z=10\%$  and with the models  $G_{d1-2}$  for the disturbances. The disturbance models are for the two input disturbances to output  $P_1$ , where each disturbance has been evaluated separately. In figure 4.1b Bode magnitude plot for operating point  $Z=30\%$  is shown and the instability is faster.

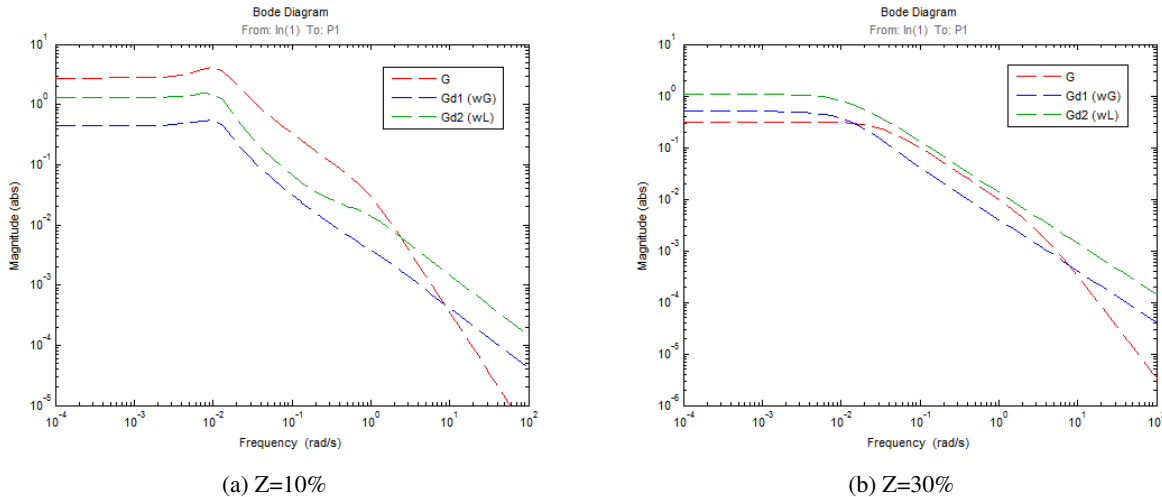


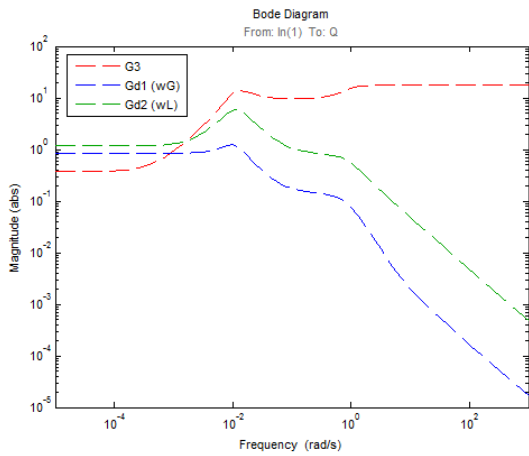
Figure 4.1: Frequency dependent gain for  $P_1$  at operating point  $Z=10\%$  and  $Z=30\%$

In figure 4.1a the process gain is higher than the disturbance gains for frequencies up to about 3 rad/s. Above this frequency the disturbance gains are lower than one and disturbance rejection is not strictly needed. For a more unstable process, as given in figure 4.1b where  $Z=30\%$ , the process gain is smaller than the disturbance gain at low frequencies. The disturbance gain for  $w_{L,in}$  is larger than one, so this will make some problems when stabilizing control is used. When disturbance gain are greater than one and larger than the process gain, the disturbance will drive the operation into a point where the controller no longer manage to stabilize the process.

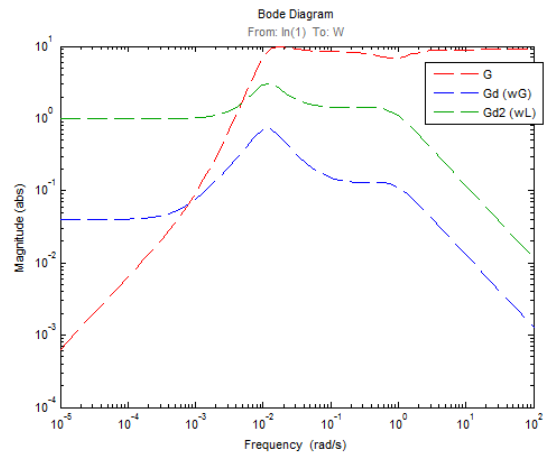
### 4.4.4 Controllability analysis of flow control

The problem with flow control,  $Q$  or  $W$  as measurements, is low steady state gain. In figure 4.2a and 4.2b Bode magnitude plot of the linear scaled process models  $G(s)$  and  $G_{d(1-2)}$  are given, obtained at an operating point  $Z=10\%$  for both  $Q$  and  $W$ .

For volumetric flow rate,  $|G| < |G_d|$  for frequencies  $< 0,001$  rad/s. When the frequencies are higher than  $0,001$ rad/s  $|G| > |G_d|$ , and flow disturbances are effectively damped through the pipeline for frequencies  $> 0,01$ . If  $Q$  is chosen as the primary controlled variable, the controller will not be able to suppress low-frequency disturbances, because of a higher disturbance gain. In this case  $Q$  should be used in the inner-loop



(a) Volumetric flow rate



(b) Mass flow rate

Figure 4.2: Frequency dependent gain for  $Q$  and  $W$  at operating point  $Z=10\%$

in a cascade controller with  $P_1$  in the outer-loop. Considering mass flow rate, disturbance gain is higher than the process gain, for frequencies  $< 0,006$  rad/s. The results are the same for  $W$  as it was for  $Q$ , the controller will not be able to suppress low-frequency disturbances. As  $W$  also has a close-to-zero steady state gain it should not be used in a single-loop control.

## 5 Controllability analysis on a three state model

A controllability analysis was performed for a three state simplified dynamic model, made by Espen Storakaas [2]. The three states used in this model are listed below.

- $m_L$ : mass of liquid in the riser and around the low-point.
- $m_{G1}$ : mass of gas in the feed section.
- $m_{G2}$ : mass of gas in the riser.

This simplified three-state model contains four empirical parameters that can be used to tune the model. For this model the bifurcation point were identified at  $Z=13\%$ , and riser slugging will only occur for  $Z > 13\%$ . This is different from the simplified four state model made by Esmail Jahanshahi. The reason for this is not clear, but it could be because the three state model was tuned after a OLGA simulation that was not so accurate. When simulating in OLGA the pipeline can be "divided" into a number of segments, increasing the number of segments will give a more accurate simulation, but it will take longer time. Espen Storakaas used a significant lower number of segments for each pipeline in the simulation, compared to what Esmail Jahanshahi used.

A controllability analysis has been performed for the three state model and in the following study, two different operating points are used. The first one is for  $Z=15\%$  where the instability is fairly slow, and the second one for  $Z=30\%$  where the instability is faster. This is the same controllability analysis used on the new model in section 4. Outputs available from this model is  $P_1$ ,  $P_2$  and  $W$ . The linearization file, model file and the initialize file have been made by Esmail Jahanshahi. The scaling used on the new model was used on the three state model, see section 4.2. RHP-poles and RHP-zeros for the two operating points are given in table 5.1, for the topside pressure. As topside pressure is the only measurement that introduce RHP-zeros into the system. The system has RHP-poles for  $Z > 13\%$ .

Table 5.1: Topside pressure: Zeros and poles

Choke valve opening (Z)	Pole 1	Pole 2	RHP-zero 1	RHP-zero 2
15%	0,0132 + 0,0134i	0,0132 - 0,0134i	1,0785	0,0122
30%	0,0882	0,0141	1,0915	0,0121

The controllability data for  $Z=15\%$  are given in tabel 5.2 for both method 1 and 2. The controllability data for  $Z=30\%$  are given in tabel 5.3 for both method 1 and 2. These results are for a constant inlet flow of 9 kg/s.

Results from this controllability analysis gives actually the same results as the analysis for the new model in section 4.4. The topside pressure should not be used as measurement for stabilizing control because of the high peaks for  $|S|$  and  $|SG|$ . The mass flow rate has a lower steady state gain than the other measurements, and should not be used alone in a single-loop control. Inlet pressure is the most suited measurement for stabilizing control, with largest steady state gain and all peaks small. For large choke valve openings it becomes more difficult to stabilize the system, as the input magnitude given by  $\|KS\|_\infty$  and  $\|KSG_{d1}\|_\infty$  exceed unity for  $P_1$ .

Table 5.2: Results from method 1 and method 2, Z=15%

Measurement	G(0)	$ S = T $	$ KS $	$ KSG_{d1} $	$ KSG_{d2} $	$ SG $	$ SG_{d1} $	$ SG_{d2} $
P <sub>1</sub> (method 1)	1,2182	1	0,6922	0,1758	0,1857	0	0	0
P <sub>1</sub> (method 2)	1,2182	1	0,8585	0,3937	0,2639	0	0	0
P <sub>2</sub> (method 1)	1,1530	4,5623	2,2563	0,1758	0,2968	4,5204	0,3079	0,5677
P <sub>2</sub> (method 2)	1,1530	4,6280	4,0592	0,3357	0,6002	2,3368	0,1592	0,2935
W (method 1)	0,1743	1	0,1750	0,1758	0,3176	0	0	0
W (method 2)	0,1743	1	0,2899	0,3357	0,5732	0	0	0

Table 5.3: Results from method 1 and method 2, Z=30%

Measurement	G(0)	$ S = T $	$ KS $	$ KSG_{d1} $	$ KSG_{d2} $	$ SG $	$ SG_{d1} $	$ SG_{d2} $
P <sub>1</sub> (method 1)	0.3069	1	3,8032	0,92288	0,61364	0	0	0
P <sub>1</sub> (method 2)	0.3069	1	4,0815	1,314	0,74158	0	0	0
P <sub>2</sub> (method 1)	0.2903	16,7515	47,8125	0,92288	1,6679	4,6357	0,31273	0,57972
P <sub>2</sub> (method 2)	0.2903	17,0757	60,6834	1,1844	2,1676	3,5316	0,23825	0,44164
W (method 1)	0.0446	1	0,85507	0,92288	1,5269	0	0	0
W (method 2)	0.0446	1	1,0691	1,1845	1,9467	0	0	0

## 6 Anti-slug control of two-phase flow in riser and limitations in system

Control systems designed to avoid riser slugging are often called slug-controllers, and this term will first be explained. Limitations in control will be discussed, as the most available measurement ( $P_2$ ) introduce RHP-zeros into the system. It is important to know that the zeros will shift location, dependent on choke valve opening. The pole locations are independent of input and measurement, and there are RHP-poles in the system when  $Z > 5\%$ . Use of controllers will always include time delays and this will impose limitation on achievable control performance. Limitation imposed by the input and inputs constraints will be discussed, and performance requirements imposed by disturbances.

Various anti-slug controller designs and solutions have been used in this project. Previous used controllers will be mentioned. Measurements most suited for stabilizing control are an important task, and a controllability analysis has been performed. The controllers were designed in MATLAB and Simulink, and used on both linear and nonlinear model. The model used is the simple dynamic model made by Esmail Janhansahi. These simulations were used to confirm results from the analysis in the previous section. Controllers based on only topside measurements can be used, and an evaluation of the performance of these controllers compared to the controllers based on upstream measurement ( $P_1$ ) will be given. P and PI controllers, linear quadratic Gaussian (LQG) controller and a combination of Kalman filter and PI controller have been used. The Kalman filter was based on different measurements, where only using  $P_2$  was tested and a combination of  $P_2$  and  $Q$  or  $W$ . Tuning parameters for each control systems were found by using the linear model, and the same parameters were implemented on nonlinear model.

### 6.1 Anti-slug control

Stabilization of desired fluid flow regimes in pipelines are challenging and the need for control engineers in this field is large. Pipeline flow has been analyzed based on the flow-regimes that develops in the pipeline under different boundary conditions. With feedback control the boundaries can be moved and this will stabilize the flow regime where riser slugging naturally occurs. In the late 1970s the first study that applied control to the riser slugging problem was published. Over ten years later, in 1990, the use of feedback control to avoid severe slugging was proposed and applied on a test rig. The last ten to fifteen years controlled-based solutions have been of interest, and these applications have been experimental or based on simulations with commercial simulators such as OLGA. Controllers have the same objective independent of design, and this is to keep the process stable such that the system does not drift too far away from its nominal operating points when disturbance and noise occur. Controllers that are designed to avoid riser slugging in riser systems are often called slug controllers. This could be a misleading term. The name "slug controller" sounds like that riser slugs still exist in the pipeline and that the controller is only trying to limit or reduce them. Controller system chosen, should completely remove riser slugs by stabilizing a desired, but unstable, flow regime that exists at the same boundary conditions as the riser slugging. [2]

A definition is given in E. Storkaas [2] for an anti-slug controller.

**Definition 1.** *An anti-slug controller is a controller that stabilizes a desired, non-oscillatory flow regime that exists at the same boundary conditions as riser slugging and thereby avoids the formation of riser slugging in the system.*

The main control objective for any stabilizing controller is to keep the process stable. This implies that the closed loop system needs to have all its poles in the left half plane to be nominal stable.

## 6.2 Limitations in system

Different sources will impose limitations on achievable control performance and controller design. These limitations will also occur in stabilization of the pipeline riser-slugging system.

### 6.2.1 Limitations imposed by inputs

An important control limitation is imposed by the input, in this case the topside choke valve (Z). The choke is located at the top of the riser and is the actuator in the process. The design of the choke is important in control. The goal will be to design a choke that is fast enough to achieve the control targets. The choke should not be too fast, because of safety reasons. Safety restrictions have to be considered because if the valve open quickly at a time when the pressure-drop over the valve is high, the flow into the separator would increase significant. This can result in overfilling the separator and it can cause an over-pressure. Input rate limitations are therefore important to consider. [2]

Inputs in a real process have constraints, and these constraints are often on the equipment used to manipulate the process. An easy example is to use a valve. This cannot be more than 100% open or fully closed. If the input reaches one of its constraints it will saturate. Saturation is reached when the controller asks for a larger or smaller value than the biggest or the smallest possible input. When input saturates the feedback path is broken [12]. A PID controller does not know anything about the constraints at the input, and this could be a problem. The model used in analysis is scaled (see chapter 4.2), so at any time  $|u(t)| \leq 1$  is required. The goal is maintaining  $|u(t)| \leq 1$  while expected disturbances are rejected and the reference change is tracked. Perfect control ( $e=0$ ) will not be considered because perfect control is never really required [3]. Acceptable control will be looked at, where  $|e| < 1$  and  $e$  is the control error. For disturbance rejection it is required that  $|G| > |G_d| - 1$  at frequencies where  $|G_d| > 1$  [3]. The bode plots for the process gain and disturbance gains are given in section 4.4.3 and 4.4.4. For low frequencies the inlet pressure should be used for stabilizing control, and it can be used in combination with  $Q$  in a cascade control system.

With large disturbances and much noise in the system, stabilization with feedback control is more difficult. To achieve  $|u| < 1$  for  $|d| = 1$  it is required that  $|G_s(p)| > |G_{d,ms}(p)|$  [3]. This requirement is for stabilization of a plant with a real RHP-pole, so this should not be used for this system. For the general case, with multiple unstable poles the following conditions are exact:  $\underline{\sigma}_H^{-1}(v(G_{d,ms}^{-1}G)) \leq 1$  [2]. When Z=10%, this condition is achieved for both inlet- and topside pressure.

### 6.2.2 Limitations imposed by RHP-zeros

RHP-zero is common in practical multivariable problems. Topside pressure as measurement introduces RHP-zeros into the riser slugging system, and these will give limitations on control. If there are RHP-zero at low frequency and the goal is tight control, the upper bandwidth is limited to  $\frac{|z|}{2}$ , approximately. For tight control on high frequencies with RHP-zero, the lower bandwidth is limited to  $2|z|$ . The bandwidth is here defined as the frequency range  $[\omega_1, \omega_2]$  over which control is effective. The control is effective if there are obtained some benefit in terms of performance. The time constant of the unstable system decide where effective control is wanted. This will depend on operating point used for the riser slugging model, as

both RHP-zeros and RHP-poles change location when  $Z$  changes. A RHP-zero will pose control limitations either at low or high frequency. The fundamental constraint on the sensitivity function for internal stability is given as  $S(z)=1$ . This is a problem since it is not compatible with the desire to have  $|S|$  small, compared to 1 when the goal is to have good output performance. Presences of RHP-zeros are therefore expected to give limitations in terms of the achievable output performance. [3]

Topside pressure has high peak values on sensitivity function when  $Z > 5\%$ , because this measurement has RHP-zeros. The RHP-zeros are getting closer to the RHP-poles when the choke valve opening increase, which increase peak value on sensitivity function. A plot of the sensitivity function is given in figure 6.1 for  $P_2$ . This plot confirm that  $P_2$  should not be used as measurement for anti-slug control, as peak values increase rapidly.

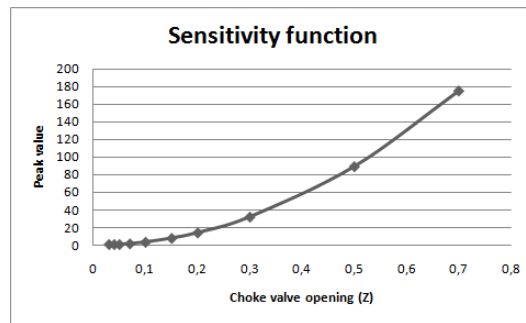


Figure 6.1: Peak values for  $|S|$ , with topside pressure as measurement

### 6.2.3 Limitations imposed by time delay

Time delays always exist in real riser slugging process, but it have not been considered much in this project. When transfer functions are found in MATLAB they lack time delay, but it could have been included. It was decided not to consider time delays other than in this section. A step test on the nonlinear model was done in Simulink, and the time delays were found for three of the measurements. Time delays normally introduce limitations in the system for both SISO and MIMO systems, but there are exceptions [3]. Time delays for the different measurements are given in table 6.1, and this is for a step test after 100 s with change in  $Z$  from 4% to 5%. This was performed on the nonlinear model in Simulink.

Table 6.1: Time delays for three measurements

Measurement	Time delay [s]
$P_1$	20
$P_2$	48
Q	10

A small effective time delay is required for good controllability, and inlet pressure has a smaller delay than the topside pressure. For a system with single RHP-pole,  $\min_K \|T\|_\infty = M_{T,\min} = M_{pz,j} \cdot |e^{p\theta}|$ , is tight. This

bound also impose a bound on the peak of  $S$  for plants with time delay. This because  $|S|$  and  $|T|$  differ by at most 1, so  $\|S\|_\infty \geq \|T\|_\infty - 1$  [3]. Time delays would have results in higher peaks on the sensitivity function, then does given in this report.

#### 6.2.4 Limitations imposed by RHP-poles

Unstable (RHP) poles will give limitations. If a system has RHP-poles, feedback control is required. This is because it is impossible to stabilize a system with feed forward control, even with a perfect model. The question is; will RHP-poles make problems for feedback control? The fundamental constraint on the sensitivity function for internal stability is given as  $S(p)=0$  [3]. This requirement will not pose a problem, because it is compatible with good output performance. The problem with the RHP-poles is something else, and the problem is at the plant input. When feedback control is used for stabilization of an unstable system, active use of system inputs are important. Minimum input usage is therefore required for an unstable plant. RHP-poles will impose a lower bound on the bandwidth and cause overshoot in the output signal. For systems that has RHP-poles, RHP-zeros and time delays, stabilization become logical more difficult and the peak values on the transfer functions are greater. The system may go unstable before the engineers have time to react. The transfer function  $KS$  can therefore be used to study the RHP-pole limitations on input usage. This is done in the controllability analysis (section 4), where a large value of  $\|KS\|_\infty$  is likely to cause saturation in  $u$  and stabilization becomes difficult [3].

The peak value on closed-loop transfer function  $KS$  starts to get large when  $Z > 10\%$ , for  $P_2$  as measurement. This exceed one for all measurements considered in the analysis when  $Z \geq 15\%$ , and controllability limitations will start to get noticeable, because of the RHP-poles.

#### 6.2.5 Performance requirements imposed by disturbances

Disturbances should also be considered when talking about performance and tight control. A system with  $|G_d(jw)| < 1$  at all frequencies do not need control, and the system is said to be self-regulating. If  $|G_d(jw)| > 1$  at some frequency, control have to be used, and normally this is feedback control. The performance requirement  $|e(w)| < 1$  for any  $|d(w)| \leq 1$  at any frequency is satisfied only if

$$|S(jw)| < \frac{1}{|G_d(jw)|}, \forall w \quad (6.1)$$

The Bode magnitude plots considered in section 4.4.3 and 4.4.4 shows that  $|G_d(jw)| > 1$  at low frequencies, with a operating point  $Z=10\%$ . The disturbance gains increase when  $Z$  increase, and process gain decrease when  $Z$  increase. This was found by plotting Bode magnitude plots for different operating points. If a system has RHP-zero at  $s=z$ , then a necessary condition for satisfying  $\|SG_d\|_\infty < 1$  is  $|G_d(z)| < 1$  [3]. Results from controllability analysis evaluating  $P_2$  give  $\|SG_d\|_\infty > 1$  and  $|G_d(z)| \approx 16$  for both disturbances, when  $Z=10\%$ .

#### Comment

It should be mentioned that the limitations given for a SISO system, is almost the same for MIMO systems. The difference with MIMO systems is that the poles and zeros have directions. So the limitations from e.g. RHP-zeros and RHP-poles are only serious in particular directions. For MIMO systems the deteriorating

effect of a RHP-zero can be moved to a less important output [3].

### 6.3 Anti-slug control of two-phase flow in riser

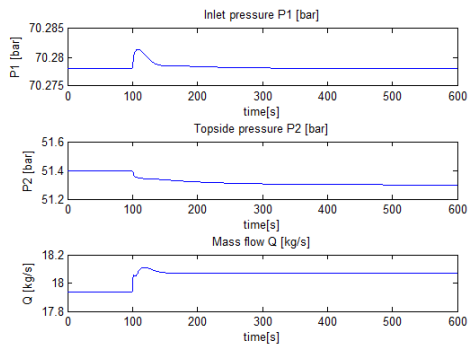
The objective for anti-slug control is to stabilize the non-oscillatory flow regime using the valve position  $Z$  as a manipulated variable. The controllability analysis already performed, concluded that the inlet pressure is the measurement most suited for stabilizing control. The analysis also gave that it should be possible to stabilize the system using a flow measurement at the pipeline outlet ( $Q$  and  $W$ ). The problem is that the inlet pressure measurement is not always available or reliable, and the flow measurements give problems with low-frequency performance. A topside pressure measurement is more available, but due to RHP-zeros and poles dynamic,  $P_2$  is probably difficult to use for stabilizing control. Results from the analysis show that a combination of  $P_2$  and  $Q$  is better to use (SIMO control system), as the minimum peak on sensitivity function is smaller than the SISO control system with  $P_2$  as measurement. The linear model is state-observable and this was found with "obsv" function in MATLAB. A state observer may be possible to use for stabilizing control, as single-loop PI controller can be difficult when topside measurements are used. The idea is therefore to use Kalman filter based on  $P_2$  and a combination of  $P_2$  and  $W$  or  $Q$ .

Different control design and solutions were used on both linear and nonlinear model in Simulink. Tuning parameters for the different controllers were found by using the linear model, and same parameters were used on nonlinear model.

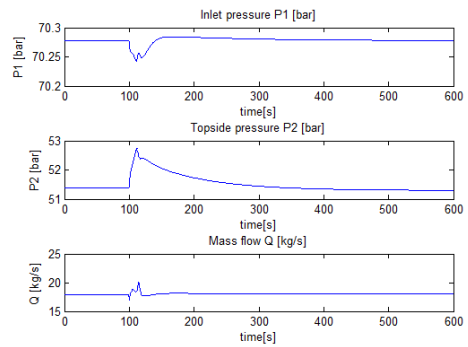
#### 6.3.1 Single-loop stabilizing control

Single-loop stabilizing control of pipeline-riser systems was tested, and a PI controller was used. First the inlet pressure was used as measurement, second the volumetric flow rate and at last topside pressure was used as measurements. A PI controller based on the inlet pressure performed well when tuning parameters were found by using SIMC tuning rule. Controller gain used was  $K_c=0,5 \text{ bar}^{-1}$  and integral time  $\tau_i = 16s$ , and the linear model obtained from linearizing around the operating point  $Z=10\%$ . Control tuning parameters found for the linear model was used on the nonlinear model. See figure 6.2a and 6.2b for stabilizing control after a change in  $w_{L,in}$  after 100 s, for linear and nonlinear model. Inlet pressure is a measurement that is well suited for stabilizing control, and it provided excellent performance on both the linear and nonlinear model. A PI controller with  $P_1$  as measurement was tested with  $Z=30\%$  and instability is faster and stabilization is more difficult. This controller still managed to stabilize the system. When the controller was taken out of action, the system became unstable extremely fast.

A P-controller was used with volumetric flow rate as measurement for stabilizing control on the linear and nonlinear model, by using tuning parameters from the linear model ( $K_c=120$ ). The result can be seen in figure 6.3a for the linear model and in figure 6.3b for the nonlinear model, with  $Z=10\%$ . A change in  $w_{L,in}$  of 0,1 kg/s was performed after 100 s. The flow controller was able to stabilize the system. The response is slow and probably new disturbances and noise will occur in the system before this controller manages to stabilize the system. With a larger step change in disturbance this controller did not manage to stabilize the system (0,5 kg/s), but the PI-controller with inlet pressure as measurement managed to stabilize with greater disturbance change.

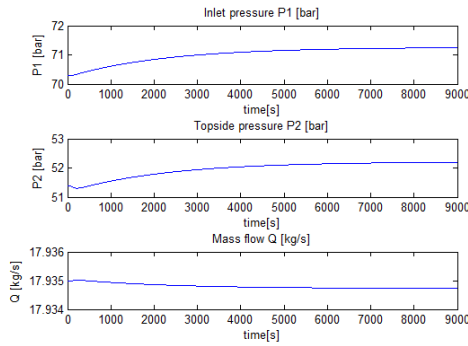


(a) Linear model

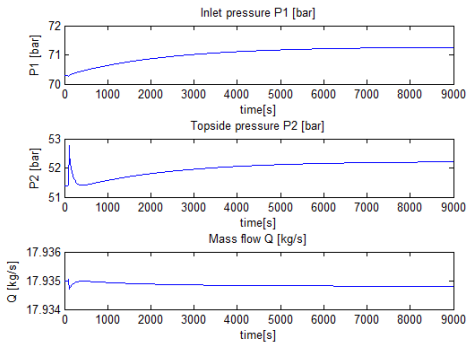


(b) Nonlinear model

Figure 6.2: Stabilizing control on linear and nonlinear model,  $P_1$  as measurements and  $Z=10\%$



(a) Linear model



(b) Nonlinear model

Figure 6.3: Stabilizing control on linear and nonlinear model,  $Q$  as measurements and  $Z=10\%$

It was not possible to stabilize the system with the topside pressure as measurement using single-loop control. Different tuning parameters and both P, PI and PID controllers were tested for stabilizing control with  $P_2$  as measurement, but still it did not manage to stabilize the system. As  $W$  has already been concluded to be used in combination with other measurements, as the steady state gain is close to zero, this was not used in a single-loop control system. Decentralized single-loop control is only possible to use for stabilizing control if suited measurements are available and reliable.

### 6.3.2 Kalman filter

The idea in this section is to use a Kalman filter to estimate the states ( $\hat{x}$ ) and measurements ( $\hat{y}$ ). A Kalman filter is a set of mathematical equations that provides an computational means to estimate states of a process, by using outputs ( $y$ ) and inputs ( $u$ ). The input is topside choke valve  $Z$  and outputs are  $P_1$ ,  $P_2$  and  $Q$  or  $W$ . Controlled variables can be measured and used individual or in combinations in the filter. The filter minimizes the mean of the squared error, and it is well known because it supports estimations of past, present and future states [13]. Another positive aspect of the filter is that it can predict states even when the precise nature of the modeled system is unknown. The Kalman filter used (`kalman.m` in MATLAB) was for a continuous time estimation, based on a linear model. The filter gain  $K_f$  was computed with the MATLAB function `kalman.m`, based on 2% variance for the process noise and 2% variance for the measurement noise ( $QN$  and  $RN$ ). An explanation of how to use this function and how a Kalman filter estimates the states can be found in appendix D. A figure of the filter made in Simulink is also attached. A Kalman filter based on topside measurements will be studied and of most interest as these measurements are most available.

The Kalman filter estimates values for the four states and values for the measurements. Estimation of  $P_1$  ( $\hat{P}_1$ ) is given in figure 6.4a for the linear model, and in figure 6.4b for the nonlinear model, with  $Z=3\%$  (stable system). These two figures show a step change in  $w_{L,in}$  after 500 s, with a Kalman filter based on the measurements  $P_2$  and  $Q$ . The two figures 6.4a and 6.4b show that estimation is difficult when there are disturbances in the process, even though the process is stable. Deviation between estimated and real values is largest for the nonlinear model.

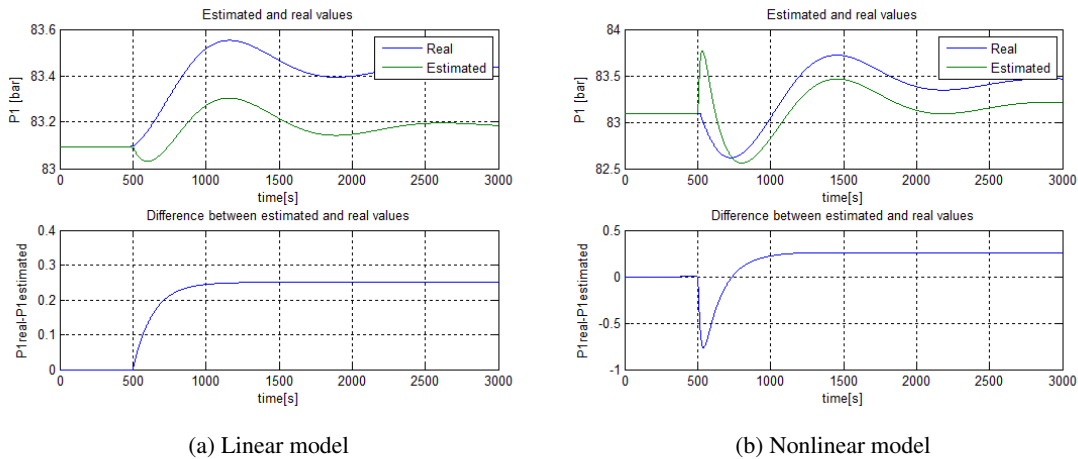


Figure 6.4: Estimation of  $P_1$ , with and  $Z=3\%$

Figure 6.5a, 6.5b, 6.5c and 6.5d give estimated values of the four states when a Kalman filter based on  $P_2$  and  $Q$  is used. This is for a linear model obtained by linearizing the simple model around operating point  $Z=10\%$ . To make some change in the system, a step change in the choke valve opening was done after 50 s (from 10 % to 11%) and a step change in  $w_{L,in}$  after 300 s. The estimation of states is good for the linear model, but there will be a deviation between real and estimated states when a disturbance occurs. The largest deviation is for  $m_{L2}$ .

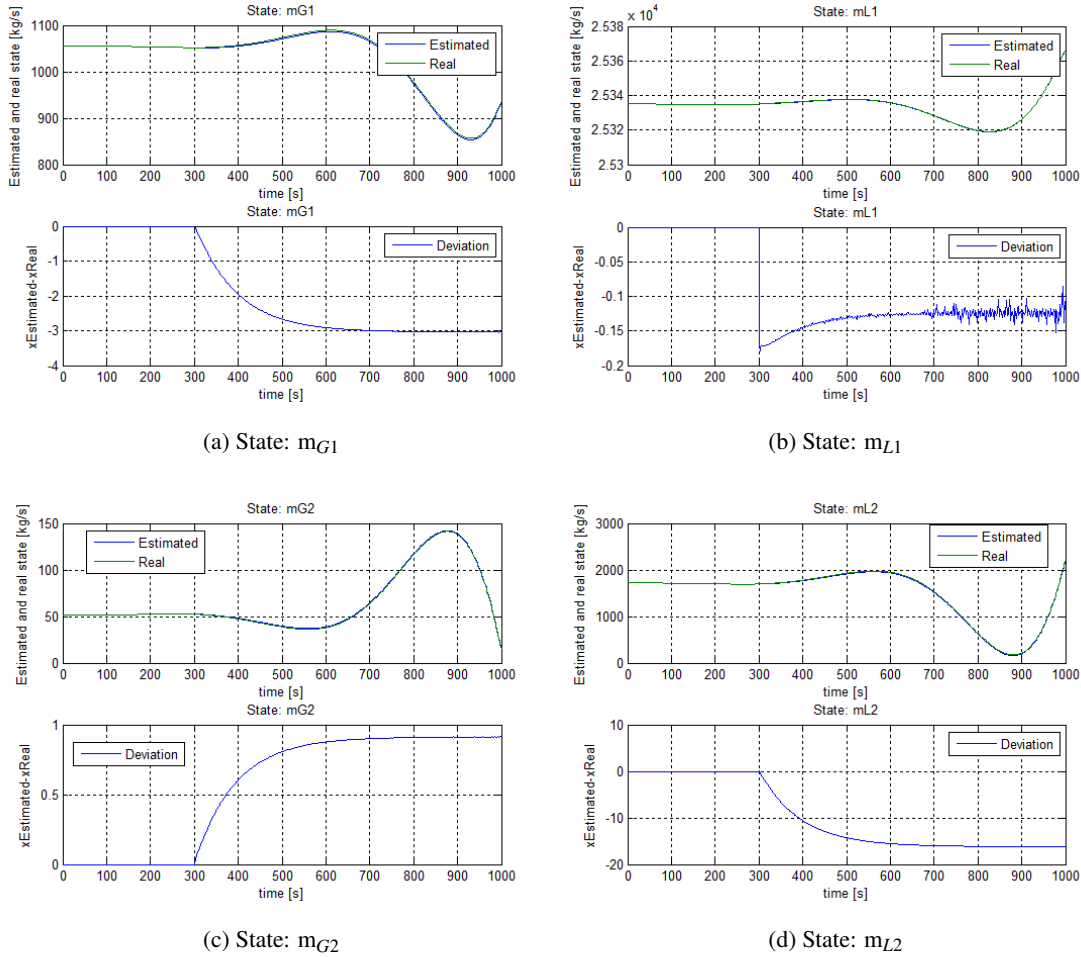
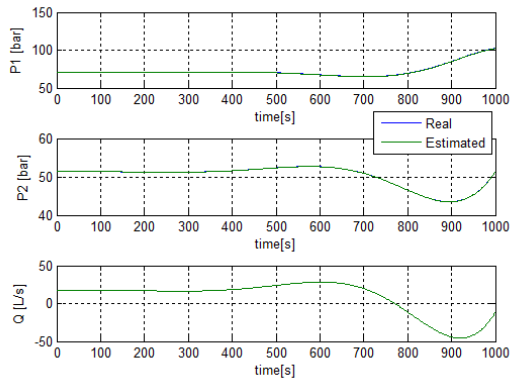
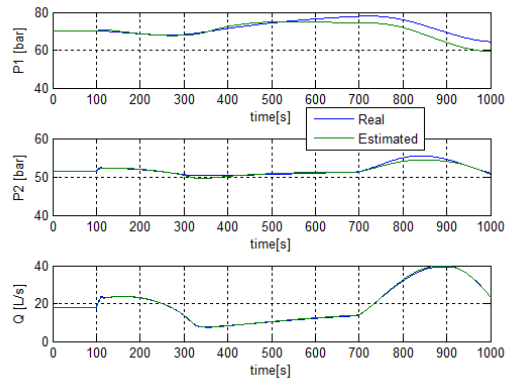


Figure 6.5: Estimation of states,  $Z=10\%$

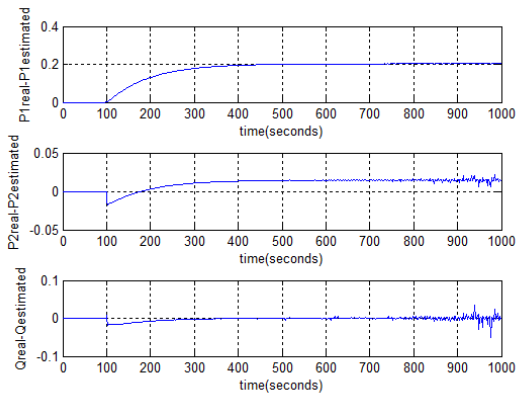
A Kalman filter based on topside measurement ( $Q$  and  $P_2$ ) with  $Z=10\%$  is further used. Real and estimated values for the measurements are shown in figure 6.6a for the linear model, and in figure 6.6b for the nonlinear model. A step change in  $w_{L,in}$  was performed after 100 s. Figure 6.6c and 6.6d shows the deviation between the estimated and real measurement values for linear and nonlinear model. These four figures shows that the estimation is best for the linear model, which is logical since this filter is based on the linear model. If the estimated measurements are used to stabilize system, this may give problems. Estimation gets more difficult when system is unstable and the Kalman filter should therefore be used in combination with e.g. optimal state feedback. As the Kalman filter used is based on the linear model it should be used carefully on the nonlinear model. For the nonlinear model a nonlinear Kalman filter could have been used, e.g. extended Kalman filter (EKF) or Unscented Kalman filter (UKF). The EKF is a widely applied state estimation algorithm for nonlinear system, but the problem is that this filter can be difficult to tune. Often the EKF gives unreliable estimates if the system nonlinearities are severe. The UKF is therefore preferred to be used because this filter reduces the linearization errors of the EKF [14]. The UKF do not use a local linearization of the nonlinear model, instead the model is directly used to propagate state estimates and probability distributions forward in time [12].



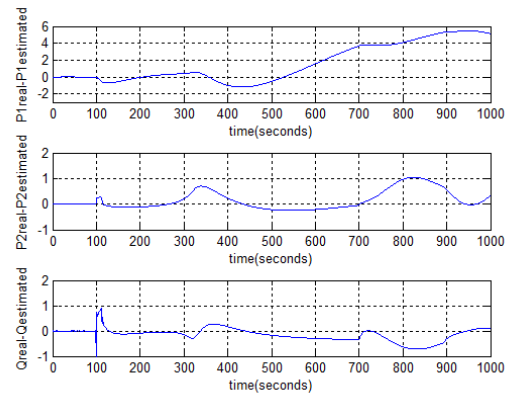
(a) Linear model



(b) Nonlinear model



(c) Deviation for linear model



(d) Deviation for nonlinear model

Figure 6.6: Real and estimated value for  $P_1$ ,  $P_2$  and  $Q$ , and deviation

### 6.3.3 Kalman filter and PI controller

A Kalman filter in combination with a PI controller was tested on both the linear and nonlinear model, for an unstable process with  $Z=10\%$ . The PI controller was tuned using SIMC-rule. First the Kalman filter was only based on topside pressure, and the estimated values of  $P_1$  ( $\hat{P}_1$ ) was used as measurement in a single-loop PI controller. This controller was not able to stabilize the linear or nonlinear model. Second a Kalman filter based on  $P_2$  in combination with  $Q$  was tested. It was only possible to stabilize the linear model in this case.

A Kalman filter made good estimations of states and measurements for the linear model, but there will be larger deviation between estimated and real values if the controller does not manage to stabilize the system. A single-loop PI controller where the estimated measurement  $\hat{P}_1$  is used, and the Kalman filter is based on topside pressure and a flow measurement, cannot be used for stabilizing control. A reason for this could be that  $P_2$  has RHP-zeros, and as these zeros will not disappear but cause problems when this control solution is used. A readily explanation can be given by looking at the two transfer functions  $P_2 = g_2(s)z(s)$  and  $P_1 = g_1(s)z(s)$ . Changing the first expression  $z(s) = g_2^{-1}P_2$ , an estimation of  $P_1$  can be given as  $\hat{P}_1 = g_1(s)g_2^{-1}P_2$ . The last expression shows that the instabilities from  $g_2$  are now in the estimated value of  $P_1$ . This controller design was not a good idea to use and a LQG controller is rather tested.

### 6.3.4 Linear-quadratic regulator (LQG)

A LQG controller is based on a known linear process model, and this model have a stochastic measurement noise  $w_n$  and disturbance signals  $w_d$  (process noise) of known variance [3]. The plant model is given in 6.2 and 6.3.

$$x' = Ax + Bu + w_d \quad (6.2)$$

$$y = Cx + Du + w_n \quad (6.3)$$

If the states are known, the LQG control problem is to find the optimal control  $u(t)$  which minimizes the optimization function 6.4. Here  $Q$  and  $R$  are chosen constant weighting matrices, which are design parameters in LQG control.

$$J = \int_0^{\infty} (x(t)^T Q x(t) + u(t)^T R u(t)) dt \quad (6.4)$$

The solution to this problem can be given as a simple state feedback law 6.5. Here  $K_r$  is the controller gain and this is found by solving an algebraic Riccati equation[2]. If the states ( $x$ ) cannot be measured, the states can be obtained from a Kalman filter. The filter gain  $K_f$  in the Kalman filter can be found by using the Riccati equation, and this has been done in section 6.3.2 and appendix D. The filter gain depend on the statically properties of the noise signals [2]. The combination of a Kalman filter and optimal state feedback is called a LQG controller, and an illustration of the setup is given in figure 6.7.

$$u(t) = -K_r x(t) \quad (6.5)$$

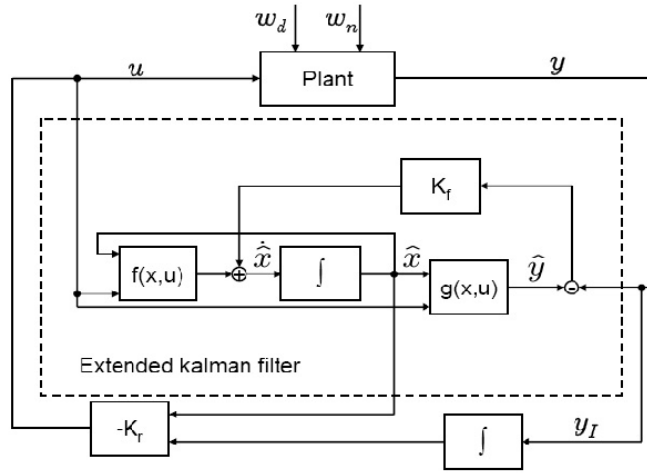


Figure 6.7: Illustration of the setup of a LQG controller[2]

The LQG controller have only proportional action, so to avoid steady-state deviations and input saturation the LQG controller can be modified by including an integrating loop (see figure 6.7). This integral loop can be chosen to only act for a subset of the measurements ( $y_I$ ). In this project a LQG controller with only proportional action was used.

### LQG controller for the pipeline-riser system

A LQG controller was used on the linear and nonlinear model, in Simulink. First a LQG controller only based on  $P_2$  was tested. Second a LQG controller based on a combination of  $P_2$  and  $W$ , and  $P_2$  and  $Q$  was designed. At last a LQG controller based on the inlet pressure and volumetric flow rate was tested. The linear model was obtained from linearizing the simplified model around the operating point for a valve opening of 10%, for every result given in this section. The filter gain  $K_f$  was computed using the MATLAB function *kalman.m*, based on 2% variance for the process noise and 2% variance for the measurement noise. The controller gain  $K_r$  was computed using the MATLAB function *lqr.m*. The weighting matrices ( $Q_n$  and  $R_n$ ) were found by starting with two identity matrices, that gave a slow response and it took around 7000 s to reach steady state. As the states are not scaled, they have a higher numerical value than the input  $u$ , so the  $R_n$  weighting matrix was multiplied with a higher number ( $10^6$ ). A faster response was achieved and steady state was reached after 1000-1500 s when weighting matrix  $R_n$  was changed. These weighting matrices were used further, by only small change in some of the simulations. The weighting matrices  $R_n$  and  $Q_n$  are given in 6.6 and 6.7. The constant  $n$  was set to 1 and 0.1, dependent of how much disturbances it were in the system and measurements used.

$$R_n = 10^6 [1] \quad (6.6)$$

$$Qn = n \cdot \begin{bmatrix} 1 & 0 \\ 0 & 1 \end{bmatrix} \quad (6.7)$$

A LQG controller based on only topside pressure was able to stabilize the linear model, but not the nonlinear model. This was after a step change in the liquid flow rate disturbance ( $w_{L,in}$ ) and  $Z=10\%$ . A LQG controller based on a combination of  $P_2$  and  $Q$  or  $W$ , was tested. The combination of using  $P_2$  and  $W$  gave only stabilizing control for the linear model. LQG controller based on a combination of  $P_2$  and  $Q$  stabilized the system for both linear and nonlinear model, with a step change in liquid inlet flow rate of 1kg/s. Figure 6.8a shows stabilization of the nonlinear model with a LQG controller, where a disturbance occur after 200 s and the controller is already active. Figure 6.8b shows a disturbance when the controller first is inactive, turned on after 5000s, and manage to stabilize the system. The LQG controller based on  $P_2$  and  $Q$  was able to stabilize the system, but the estimations of the measurements are not exact and a deviation occur specially for  $P_1$ . It can be seen from both figures that the controller does not manage to bring pressures back to reference values, and the same results occur for smaller disturbance changes. An integrating loop action should have been implemented to avoid steady state offset.

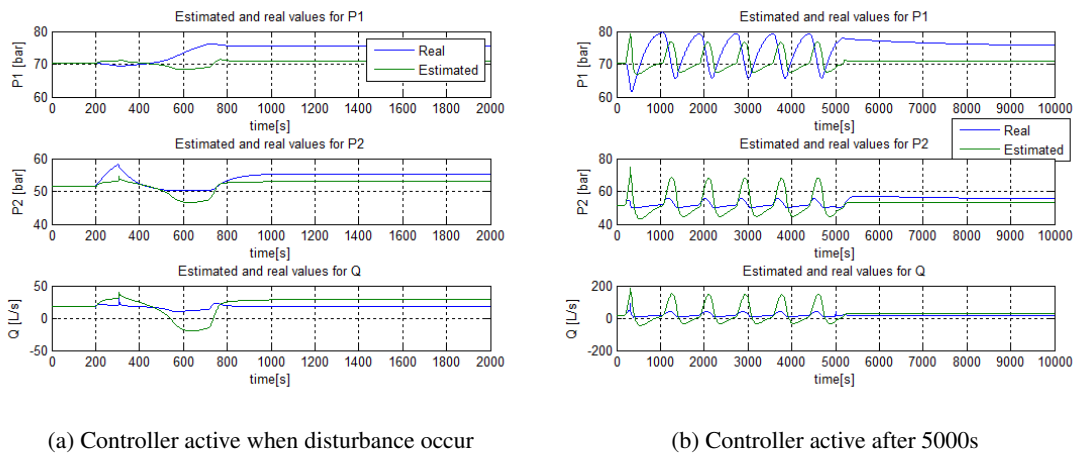


Figure 6.8: LQG controller based on measurement  $P_2$  and  $Q$ , used on nonlinear model

By curiosity and for comparison, a LQG controller based on inlet pressure and volumetric flow rate was tested. If inlet pressure is available and can be used as measurement, a PI controller will make stabilizing control, so it is unlikely that a LQG controller will improve the performance. Figure 6.9a shows stabilization of the nonlinear model with a LQG controller based on  $P_1$  and  $Q$ , where a disturbance occur after 200 s and the controller is already active. Figure 6.9b shows a disturbance when controller is inactive, and then turned on after 5000s. The LQG controller manages to stabilize the system in both situations.

The last LQG controller based on inlet pressure and topside volumetric manage to stabilize the system most rapid, and the deviation between real and estimated measurements values are smaller. A LQG controller based on topside pressure have some limitation in the estimation, that could be a result of the RHP-zero. If only topside measurements are available, a combination of topside pressure and volumetric flow rate should be used instead of only topside pressure. Controllability analysis has actually already confirmed that

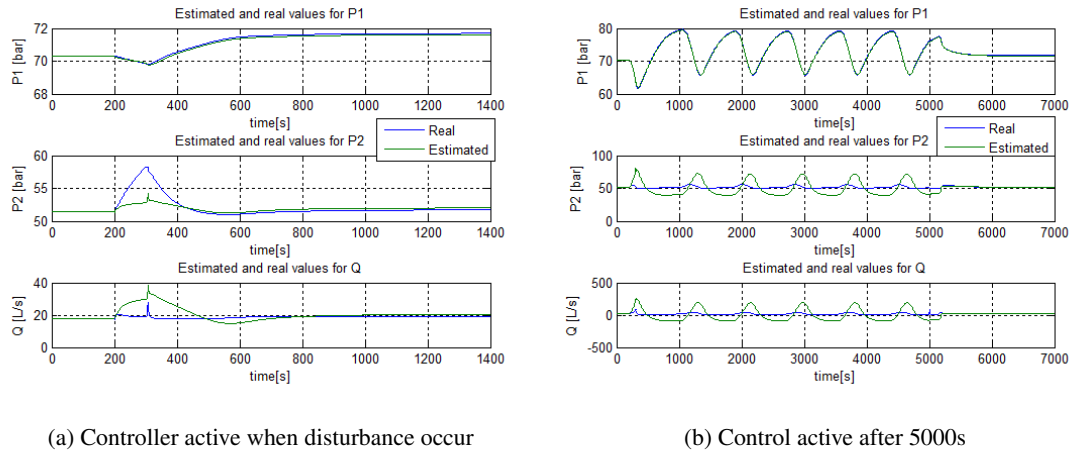


Figure 6.9: LQG controller based on measurement  $P_1$  and  $Q$ , used on nonlinear model

a combination is better, so this strengthen the result in analysis. As there is steady state offset independent of measurements the LQG controller is based on, an integrating loop action should have been implemented. None of the LQG controllers were able to bring pressures back to reference value, but the LQG controller based on inlet pressure instead of topside pressure had the smallest steady state offset. Stabilization of the linear model in Simulink with a LQG controller did also give a steady state offset. The results for linear model are not shown here, but deviation between real and estimated values were smaller for the linear model than the nonlinear model. This is probably because the Kalman filter is based on the linear model. A reason for deviation in state estimation of the linear Kalman filter could be because estimation was done around a limit cycle that is too far from the operating point. The estimation of  $m_{L2}$  is the state with largest deviation when a LQG controller based on  $P_2$  and  $Q$  was used on the linear model. Improvements can be to implement a nonlinear Kalman filter and it is recommended to use an Unscented Kalman filter with the nonlinear model.

A short comment about noise in the simulations should be given. When controllers were designed in Simulink, noise was not implemented. Both input- and measurement noise could, and actually should have been used. If noise had been used the simulation would probably be more close to the reality and stabilization of the system had become more difficult. For further work, noise should be used.

## 6.4 Previous controller methods used on riser slugging

Model-based anti-slug controllers have been studied by others. Espen Storkaas [2] used the controller design already performed in this project, but also  $H_\infty$  controllers and cascade control. These controller designs were used on a three state model.

$H_\infty$  optimization is a method used to design robust controllers. The method finds the controller  $K$  that minimizes the maximum singular value ( $H_\infty$  norm) of one or more (weighted) closed loop transfer functions. This will maximize the robustness and, by using the weights, shaping a closed loop response. A general control configuration is given in figure 6.10.

The  $H_\infty$  optimization can be used to minimize the worst case error signal  $z$ , for all exogenous signals  $w$  [2].

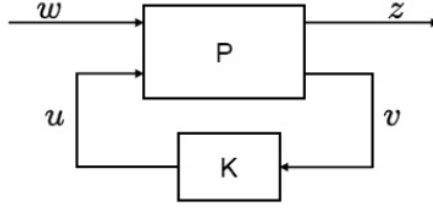


Figure 6.10: General control configuration[3]

The exogenous signals  $w$  can include both disturbances ( $d$ ), commands ( $r$ ) and measurement noise ( $n$ ). The process in figure 6.10 can be described by the matrices given in equation 6.8 and 6.9.

$$\begin{bmatrix} z \\ v \end{bmatrix} = P(s) \begin{bmatrix} w \\ u \end{bmatrix} = \begin{bmatrix} P_{11} & P_{12} \\ P_{21} & P_{22} \end{bmatrix} \begin{bmatrix} w \\ u \end{bmatrix} \quad (6.8)$$

$$u = K(s)v \quad (6.9)$$

As can be seen in figure 6.10,  $u$  is the control variables and  $v$  is the measured variables. The goal here is to find a controller(s)  $K$  that minimizes the function in equation 6.10.  $F_l(P,K)$  is the linear fractional transformation for the system [2].

$$\|F_l(P,K)\|_\infty \triangleq \max_w \bar{\sigma}(F_l(P,K)(jw)) \quad (6.10)$$

where

$$F_l(P,K) = P_{11} + P_{12}K(I - P_{22}K)^{-1}P_{21} \quad (6.11)$$

The  $H_\infty$  controller design did stabilize the flow, with a small input usage and quick and accurate setpoint tracking. The results were different, depending on which measurements that were used. [2]

Model predictive control (MPC) is also a possible control solution that could have been used. The basic MPC concept will be shortly explained. MIMO processes can be controlled while satisfying inequality constraints on the input and output variables. A reasonably accurate dynamic model of the process has to be available, and then the model and current measurements can be used to predict future values of the outputs. Changes in the inputs variables can then be calculated based on both predictions and measurements. The dynamic model for MPC can be both a physical model and an empirical model. Nonlinear and linear model can be used. There are plenty literature available on MPC. [15]

Cascade control has also been used for stabilizing control. Combinations of both  $P_1$  and  $Q$ , and  $P_2$  and  $Q$  haven been used in cascade control. It was found that a flow measurement should not be used alone in a single-loop stabilizing control.  $Q$  should be in the inner loop and  $P_1$  and  $P_2$  can be used in the outer loop. As seen from the bode plots for the different measurements (see section 4.4.3 and 4.4.4), they have advantages in different frequency ranges and that is the reason for using cascade.

## 7 Conclusion and further work

### 7.1 Conclusion

Slugging is a serious problem in multiphase pipelines, and different efforts have been made in order to prevent the problem. Slug control has been tested by using different controller design based on different measurements. These controllers used the topside choke as the manipulated variable, and measurements that have been considered are inlet pressure, topside pressure, volumetric flow rate and mass flow rate. The last three are topside measurements. Not all these measurements are suited to be used for stabilizing control, and which one to use had to be found by analysis. A simple dynamic model for riser slugging systems has been used to perform a controllability analysis that calculate minimum peaks for the closed-loop transfer function  $S$ ,  $KS$ ,  $SG$ ,  $SG_d$  and  $KSG_d$ . The results from this analysis were that inlet pressure was best suited as measurement for stabilizing control. Flow measurements ( $Q$  and  $W$ ) could be used for stabilizing control, but due to low steady-state gain, they should only be used in an inner loop cascade controller or in a combination with other measurements. Topside pressure was the only measurement that introduces RHP-zeros into the system, and these RHP-zeros get closer to the RHP-poles when the choke valve opening increase. Topside pressure was not suited as measurement for stabilizing control because of high peaks for all closed-loop transfer functions in analysis. A combination of topside pressure and volumetric flow rate was more reliable for stabilization of the system, than using them separately. This was seen by evaluating the peak values for the closed-loop transfer function  $S$  and  $KS$ .

Different sources imposed limitations on achievable control performance and controller design. A combination of RHP-zeros, RHP-poles, time delays, disturbances and input constraints made control more difficult. This system had RHP-poles when the choke valve opening was greater than 5% and the topside pressure introduced RHP-zeros into the system. No matter what controller design used, the effect of an input change on the output was delayed by the time  $\theta$ . Inlet mass flow rate are disturbances, where liquid and gas were used as two disturbances. As these two changed, they could be able to drive the operation into a point where the controller no longer managed to stabilize the process. This may happen at low frequencies if  $Q$  and  $W$  were used as measurements for stabilizing control. As the disturbance gain exceed a magnitude one and was greater than the process gain, when  $Z=10\%$  (unstable system). For larger choke valve openings, the frequency range where disturbance gain was larger than the process gain increased. Inputs in a real process have constraints, and these constraints are often on the equipment used to manipulate the process. In this case the topside choke valve, and the design on the choke is important.

Different controller design based on different measurements for an operating point of 10% was tested, on both linear and nonlinear model in Simulink. This confirmed that inlet pressure was most suited as measurement for stabilizing control when a single-loop PI controller was used. Volumetric flow rate could also be used for stabilizing control with a single-loop PI controller, but it had a slow response and it took too long time before the system reached steady state. A LQG controller was used and estimation of states and measurements were performed by using a Kalman filter, based on a linear model and different combinations of measurements. Single and multiple measurements were used. Tuning parameters for the LQG controller were found on the linear model and the same parameters were implemented on the nonlinear model. A LQG controller based on only topside pressure was not able to stabilize the system. LQG controller based on the two measurements combinations  $P_2$  and  $Q$ , or  $P_1$  and  $Q$ , were both able to stabilize the system. The LQG controller based on inlet pressure had smallest deviation between estimated and real values for the measurements, and a smaller steady state offset. The deviations between estimated and real values were

largest for the nonlinear model. A Kalman filter based on a linear model should not have been used on the nonlinear model, and an Unscented Kalman filter could have been a better alternative. The LQG controller used had only proportional action, but to avoid steady-state deviation an integrating loop action should have been used on all measurements, or only on a subset of measurements.

## 7.2 Further work

The riser-slugging process involves many challenges and complications that makes it difficult to assess the process completely and take everything into account. The project work has been carried out over a short period of time, and without any prior experience with multiphase riser-slugging processes. There is much further work that can be done on this subject and some ideas for further work will be listed below.

- Include more noise in the Simulink simulations. Both input and measurement noise should be implemented.
- Perform a controllability analysis with other various measurements, e.g. density ( $\rho$ ) and flow out of the riser. Study more combinations of measurements that can be used in MIMO controllers. Combinations of measurements have different properties than the original measurement. Try to use flow measurements obtained from topside density and pressure, by using a valve equation.
- Perform a controllability analysis for a S-shaped riser. A simple dynamic model for this riser configuration has to be found first.
- Design a cascade controller, as the different measurements have advantages in different frequency ranges.
- Build an Unscented Kalman filter, which could be used on the nonlinear model when a LQG controller is tested or another model based controller is used.
- Make a LQG controller with integrating loop action on a subset of different measurements.
- Test both MPC and NMPC on the new riser slugging model, and for the nonlinear model use a nonlinear Kalman filter.
- Build controllers in OLGA and test them. This is possible, but it requires that OLGA is a well-known program and the person knows how to use it.

## References

- [1] D. O. Bratland, “The flow assurance site.” <http://drbratland.com/PipeFlow2/chapter1.html>, 18.September, kl.12.30 2010.
- [2] E. Storkaas, *Stabilizing control and controllability*. PhD thesis, Norwegian University of Science and Technology, 2005.
- [3] S. Skogestad and I. Postletwaite, *Multivariable Feedback Control*. West Sussex PO19 8SQ, England: John Wiley and Sons, Inc, 2005.
- [4] H. Sivertsen, *Stabilization of desired flow regimes*. PhD thesis, Norwegian University of Science and Technology, 2008.
- [5] E. Jahanshahi and S. Skogestad, “Simplified dynamical models for control of severe slugging in multiphase risers,” *Submitted to 18<sup>th</sup> IFAC World Congress. Received October 12, 2010*.
- [6] C. E. Brennen, *Fundamentals of multiphase flow*. 100 Brook Hill Drive, West Nyack, NY 10994-2133: Cambridge University Press, first edition ed., 2005.
- [7] H. Sivertsen, E. Storkaas, and S. Skogestad, “Small-scale experiments on stabilizing riser slug flow,” *Chemical engineering research and design*, vol. 88, pp. 213–228, 2010.
- [8] E. Storkaas and S. Skogestad, “Controllability analysis of two-phase pipeline-riser systems at riser slugging conditions,” *Control Engineering Practice*, vol. 15, pp. 567–581, 2007.
- [9] S. GROUP, “Olga - spt group internet.” <http://www.sptgroup.com/en/Products/olga/>, 30.September, kl.17.23 2010.
- [10] J. Chen, “Logarithmic integrals, interpolation bounds, and performance limitations in mimo feedback systems,” *IEEE TRANSACTIONS ON AUTOMATIC CONTROL*, vol. 45, pp. 1098–1115, 2000.
- [11] H. A. Preisig, “Dynamic systems and control technology, tue.” <http://www.nt.ntnu.no/users/preisig/>, 1998.
- [12] M. Hovd, “Lecture notes for the course advanced control of industrial processes.” Used in lecture at NTNU, TTK4210, November 2009.
- [13] G. Welch and G. Bishop, *An introduction to the Kalman filter*. Department of Computer Science University of North Carolina at Chapel Hill, Chapel Hill, NC 27599-3175, 2006.
- [14] D. Simon, *Optimal state estimation*. Hoboken, New Jersey: John Wiley and Sons, Ltd, second edition ed., 2006.
- [15] D. E. Seborg, T. F. Edgar, and D. A. Mellichamp, *Process Dynamics and Control*. 111 River Street, Hoboken, NJ07030: John Wiley and Sons, Ltd, second edition ed., 2004.

## A Nomenclature

Table A.1: Nomenclature

Symbol	Description	Unit
$A_G$	Free area for gass flow	$m^2$
$A_L$	Free area for gass flow	$m^2$
$\bar{h}_1$	Level of liquid in pipeline at lowpoint	m
$h_c$	Critical liquid level	m
$K_G$	Orifice coefficient for gas flow through the lowpoint	-
$K_h$	Correction factor for level of liquid in pipeline	-
$K_L$	Orifice coefficient for liquid flow through lowpoint	-
$K_{p^c}$	Choke valve constant	-
$L$	Length of pipeline	m
$M_G$	Molecular weight gas	kg/kmol
$m_{G1}$	Mass of gas in the pipeline	kg
$m_{G2}$	Mass of gas in the riser	kg
$m_{L1}$	Mass of liquid in the pipeline	kg
$\bar{m}_{L1}$	Average mass of liquid in pipeline	kg
$m_{L2}$	Mass of liquid in the riser	kg
$P_0$	Pressure after choke valve	bar
$P_1$	Inlet pressure	bar
$P_{1,nom}$	Nominal pressure	Pa
$P_2$	Topside pressure	bar
$Q$	Volumetric flow rate	L/s
$R$	Gas constant	J/(K.Kmol)
$r_1$	radius in pipeline	m
$r_2$	radius in riser	m
$Re_p$	Reynolds number	-
$T$	Temperature	K
$u$	Plant inputs (manipulated variable)	-
$\bar{U}_m$	average mixture velocity in riser	m/s
$U_{sg2}$	Average velocity of gas in riser	m/s
$U_{sl,in}$	Average velocity of liquid in inlet	m/s
$U_{sl2}$	Average velocity of liquid in riser	m/s
$V_1$	Total volume in upstream	$m^3$
$V_2$	Total volume in riser	$m^3$
$V_{G1}$	Volume occupied by gas in pipeline	$m^3$
$V_{G2}$	Volume occupied by gas in riser	$m^3$
$W$	Mass flow rate topside	kg/s
$w_{G,in}$	Inlet gas flow rate	kg/s
$w_{G,lp}$	Gas flow rate in low point	kg/s
$w_{G,out}$	Outlet gas flow rate	kg/s
$w_{L,in}$	Inlet liquid flow rate	kg/s

Continued on next page

Table A.1 – continued from previous page

Symbol	Description	Unit
$w_{L,lp}$	Liquid flow rate in lowpoint	kg/s
$w_{L,out}$	Outlet liquid flow rate	kg/s
$w_{mix}$	Two-phase mixture flow rate	kg/s
$y$	plant outputs (Controlled variables)	
$y_m$	measured $y$ (measurements)	-
$Z$	choke valve opening	%
$Z_0$	Nominal choke valve opening	-
$\alpha_L$	Liquid volume fraction	-
$\bar{\alpha}_{L1}$	Average volume fraction	
$\bar{\alpha}_{L2}$	Average liquid volume fraction in riser	
$\alpha_{Lm}$	Liquid mass fraction	-
$\alpha_{Lm,t}$	Liquid mass fraction at top	-
$\alpha_{L,t}$	Liquid volume fraction at the top of riser	-
$\Delta P_{fp}$	Pressure loss due to friction	bar
$\Delta P_{fr}$	Pressure loss due to friction in riser	bar
$\Delta P_G$	Pressure drop of the gas through orifice	bar
$\theta$	Time delay	s
$\lambda_p$	Friction factor in pipeline	-
$\lambda_r$	Friction factor in riser	-
$\mu$	Viscosity	-
$\rho_G$	Gas density	kg/m <sup>3</sup>
$\bar{\rho}_{G1}$	Average gas density	kg/m <sup>3</sup>
$\rho_{G2}$	Density of gas at top of the riser	kg/m <sup>3</sup>
$\rho_L$	Liquid density	kg/m <sup>3</sup>
$\rho_t$	Density top	kg/m <sup>3</sup>

## B The new model

This model is made by Esmail Jahanshahi [5]. The new model is using four tuning parameters, these makes the model more like the reality. These tuning parameters are the choke valve constant ( $K_{pc}$ ), a orifice coefficient for gas flow through the lowpoint ( $K_G$ ), the third one is a orifice coefficient for liquid flow through lowpoint ( $K_L$ ) and the last one is  $K_h$  that is a correction factor for level of liquid in pipeline. There are used four state variables and these are listed below. For each state variables there is a state equation and these are given in B.1, B.2, B.3 and B.4. The model was not finished when it was started to be used in the project. In the start of october the final and last version was made, and this is the one given below.

- $m_{G1}$ : Mass of gas in the pipeline
- $m_{L1}$ : Mass of liquid in the pipeline
- $m_{G2}$ : Mass of gas in the riser
- $m_{L2}$ : Mass of liquid in the riser

### B.1 State equations

$$\frac{dm_{G1}}{dt} = w_{G,in} - w_{G,lp} \quad (B.1)$$

$$\frac{dm_{L1}}{dt} = w_{L,in} - w_{L,lp} \quad (B.2)$$

$$\frac{dm_{G2}}{dt} = w_{G,lp} - w_{G,out} \quad (B.3)$$

$$\frac{dm_{L2}}{dt} = w_{L,lp} - w_{L,out} \quad (B.4)$$

### B.2 Boundary Conditions

The inlet gas and liquid mass flow rates are already given in equation B.1 and B.2, and these are assumed to be constant. The inlet boundary are not assumed constant since these are easily changed. The fraction of the liquid volume in the pipeline section is given by the liquid mass fraction and the density of the two phases B.5.

$$\alpha_L = \frac{\alpha_{Lm}/\rho_L}{\alpha_{Lm}/\rho_L + (1 - \alpha_{Lm})/\rho_G} \quad (B.5)$$

By simulation in OLGA, it was concluded that the liquid volume fraction in the pipeline section is approximately constant in time. This also applies along the pipeline except a small part at the low point. The liquid volume fraction in the pipeline section is approximated using the inflow boundary condition B.6.

$$\bar{\alpha}_{Lm1} \cong \frac{w_{L,in}}{w_{G,in} + w_{L,in}} \quad (B.6)$$

By combining B.6 and B.5 the average liquid volume fraction in the pipeline is given in equation B.27.

$$\bar{\alpha}_{L1} \cong \frac{\bar{\rho}_{G1} w_{L,in}}{\bar{\rho}_{G1} w_{L,in} + \rho_L w_{G,in}} \quad (\text{B.7})$$

The gas density  $\bar{\rho}_{G1}$  given in B.27 was found by using the steady state pressure of the pipeline B.8.

$$\bar{\rho}_{G1} = \frac{P_{1,nom} M_G}{RT_1} \quad (\text{B.8})$$

For the outflow conditions at the outlet of the riser a constant pressure in the separator and a choke valve model of two-phase flow are assumed B.9. The relative valve opening ( $Z$ ) is from 0 to 1, and  $f(z)$  is the characteristic equation of the valve. In this model it is assumed a linear valve function.

$$w_{mix,out} = K_{pc} f(z) \sqrt{\rho_t (P_{2,t} - P_0)} \quad (\text{B.9})$$

The mass flow rates of liquid ( $w_{L,out}$ ) and gas ( $w_{G,out}$ ) out of the riser is given in B.10 and B.11.

$$w_{L,out} = \alpha_{Lm,t} w_{mix,out} \quad (\text{B.10})$$

$$w_{G,out} = (1 - \alpha_{Lm,t}) w_{mix,out} \quad (\text{B.11})$$

### B.3 Pipeline model

In this part the gas and liquid are assumed to be distributed homogeneously along the pipeline (steady-state condition). The mass of liquid in the pipeline is given by  $\bar{m}_{L1} = \rho_L V_1 \bar{\alpha}_{L1}$ . The level of liquid in the pipeline at the low-point is approximated to be  $\bar{h}_1 \cong h_c \bar{\alpha}_{L1}$ . If the liquid content in the pipeline increases with  $\Delta m_{L1}$  (B.12), it starts to fill up the pipeline from the low-point. A length given by  $\Delta L$  will be occupied by only liquid, and the liquid level will be increased by  $\Delta h_1 = \Delta L \sin(\theta)$ . The level of liquid in the pipeline  $h_1$  is given in B.13 and B.15, and this gives that  $h_1$  can be given as a function of liquid mass in the pipeline  $m_{L1}$ . This is a state variable of the model, and the other parameters in B.15 are constant.

$$\Delta m_{L1} = \Delta L \pi r_1^2 (1 - \bar{\alpha}_{L1}) \rho_L \quad (\text{B.12})$$

$$h_1 = \bar{h}_1 + \Delta L \sin(\theta) = \bar{h}_1 + \frac{\Delta m_{L1}}{\pi r_1^2 (1 - \bar{\alpha}_{L1}) \rho_L} \sin(\theta) \quad (\text{B.13})$$

where

$$\bar{h}_1 = K_h h_c \bar{\alpha}_{L1} \quad (\text{B.14})$$

$$h_1 = K_h h_c \bar{\alpha}_{L1} + \left( \frac{m_{L1} - \rho_L V_1 \bar{\alpha}_{L1}}{\pi r_1^2 (1 - \bar{\alpha}_{L1}) \rho_L} \sin(\theta) \right) \quad (\text{B.15})$$

The equations prove that the liquid content in the pipeline has a direct effect on the liquid level in the pipeline. The liquid that is in excess is causing a blockage of the gas in the low point, and this gives the slug flow in

the riser. The volume that is occupied by gas in the pipeline is given in equation B.16. The gas density and pressure (assuming ideal gas) is given in equations B.17 and B.18.

$$V_{G1} = V_1 - m_{L1}/\rho_L \quad (\text{B.16})$$

$$\rho_{G1} = \frac{m_{G1}}{V_{G1}} \quad (\text{B.17})$$

$$P_1 = \frac{\rho_{G1}RT_1}{M_G} \quad (\text{B.18})$$

For pressure loss due to friction in the pipelines, the pressure loss is given in equation B.19. Here only friction of liquid is considered.

$$\Delta P_{fp} = \frac{\overline{\alpha_{L1}} \lambda_p \overline{U}_{sl,in}^2 L_1}{4r_1} \quad (\text{B.19})$$

In equation B.19  $\lambda_p$  (B.20) is the correlation for turbulent flow in smooth wall pipes, and this is used as the friction factor in the pipeline.

$$\lambda_p = 0,0056 + 0,5 \text{Re}_p^{-0,32} \quad (\text{B.20})$$

The Reynolds number is given in equation B.21. In these equation given,  $U_{sl,in}$  is superficial velocity of inlet liquid B.22.

$$\text{Re}_p = \frac{2\rho_L \overline{U}_{sl,in} r_1}{\mu} \quad (\text{B.21})$$

$$\overline{U}_{sl,in} = \frac{w_{L,in}}{2\pi r_1^2 \rho_L} \quad (\text{B.22})$$

#### B.4 Riser model

Total volume of riser B.23.

$$V_2 = A_2(L_2 + L_3) \quad (\text{B.23})$$

Volume occupied by gas in the riser B.24.

$$V_{G2} = V_2 - m_{L2}/\rho_L \quad (\text{B.24})$$

Density of gas at the top of the riser B.25.

$$\rho_{G2} = \frac{m_{G2}}{V_{G2}} \quad (\text{B.25})$$

Pressure at the top of the riser, used ideal gas law B.26.

$$P_{2,t} = \frac{\rho_{G2}RT_2}{M_G} \quad (\text{B.26})$$

The average liquid volume fraction in the riser B.27.

$$\bar{\alpha}_{L2} = \frac{m_{L2}}{V_2 \rho_L} \quad (\text{B.27})$$

The average density of the two-phase flow inside the riser B.28.

$$\bar{\rho}_2 = \frac{m_{G2} + m_{L2}}{V_2} \quad (\text{B.28})$$

The friction loss in the riser is given in equation B.29, here the friction factor of the riser is the same as for the pipeline. But it is called  $\lambda_r$ , since it is in the riser.

$$\Delta P_{fr} = \frac{\bar{\alpha}_{L2} \lambda_r \bar{\rho}_m \bar{U}_m^2 (L_2 + L_3)}{4r_2} \quad (\text{B.29})$$

The Reynolds number of the flow in riser is given in equation B.30, and the equation for the average mixture velocity is given in equation B.31, B.32 and B.33.

$$\text{Re}_r = \frac{2r_2 \bar{\rho}_m \bar{U}_m}{\mu} \quad (\text{B.30})$$

$$\bar{U}_m = \bar{U}_{sl2} + \bar{U}_{sg2} \quad (\text{B.31})$$

$$\bar{U}_{sl2} = \frac{w_{L,in}}{\pi r_2^2 \rho_L} \quad (\text{B.32})$$

$$\bar{U}_{sg2} = \frac{w_{G,in}}{\pi r_2^2 \rho_{G2}} \quad (\text{B.33})$$

## B.5 Model for the gas flow in the low point

When the liquid level ( $h$ ) in the pipeline is above the critical level ( $h_c$ ), the liquid will block the low point in the riser and the gas flow rate ( $w_{G,in}$ ) will be zero. If there are no blocking by the liquid in the low point, the gas will flow from  $V_{G1}$  to  $V_{G2}$  with mass flow rate  $w_{G,lp}$ . The most important parameters that determined the gas rate are the pressure drop (low point) and the opening are. This is found by physical insight in the system. A orifice equation can therefore be used to describe the gas transport. The pressure drop is driving the gas through the orifice that has a opening are  $A_G$ , see equation B.34.

$$w_{G,lp} = K_G A_G \sqrt{\rho_{G1} \Delta P_G}, \quad h < h_c \quad (\text{B.34})$$

where

$$\Delta P_G = P_1 - \Delta P_{fp} - P_2 - \bar{\rho}_m g L_2 - \Delta P_{fr} \quad (\text{B.35})$$

## B.6 Model for the liquid flow in the low point

The liquid mass flow rate in the low-point is also described by an orifice equation B.36. The free area for gas flow is given in B.38, and this is found by using a geometrical method.

$$w_{L,lp} = K_L A_L \sqrt{\rho_L \Delta P_L} \quad (\text{B.36})$$

where

$$\Delta P_L = P_1 - \Delta P_{fp} + \rho_L g h_1 - P_2 - \bar{\rho}_m g L_2 - \Delta P \quad (\text{B.37})$$

$$\phi = \left( \pi - \arccos \left( 1 - \frac{(h_c - h_1) \cos(\theta)}{r_1} \right) \right), \quad h < h_c \quad (\text{B.38})$$

where

$$A_G = r_1^2 (\pi - \phi - \cos(\pi - \phi) \sin(\pi - \phi)), \quad h < h_c \quad (\text{B.39})$$

A quadratic approximation of B.38 and B.39 is used in the model. These approximations are given in B.40 and B.41.

$$A_G \cong \pi r_1^2 \left( \frac{h_c - h_1}{h_c} \right)^2, \quad h_1 < h_c \quad (\text{B.40})$$

$$A_L = \pi r_1^2 - A_G \quad (\text{B.41})$$

## B.7 Phase distribution model at outlet choke valve

Gas mass fraction at the outlet choke valve B.42 and the density of two-phase flow through the outlet choke valve B.43.

$$\alpha_{Lm,t} = \frac{\alpha_{L,t} \rho_L}{\alpha_{L,t} \rho_L + (1 - \alpha_{L,t}) \rho_{G2}} \quad (\text{B.42})$$

$$\rho_t = \alpha_{L,t} \rho_L + (1 - \alpha_{L,t}) \rho_{G2} \quad (\text{B.43})$$

The volume fraction at top of the riser,  $\alpha_{L,t}$ , can be found by the entrainment model proposed by Storkaas[2]. In this model a simple approach (physical assumptions) is used in order to calculate the liquid volume fraction at the top of the riser. A simplification is used because the entrainment equations are complicated and make the model very stiff. It is used that in a vertical gravity dominant two-phase flow pipe, there is a linear relationship between pressure and liquid volume fraction. The gradient of the pressure in the riser, is assumed to be constant for the desired smooth flow regimes. The liquid volume fraction is also assumed to have a constant gradient along the riser, for the mentioned flow regimes. After simulations in OLGA and study of the profile plots of the pressure and the liquid volume fraction, it was confirmed that it could be used a constant gradient along the riser for the desired stable flow regimes B.44. This assumption suggests that the liquid volume fraction at the middle of the riser, is the average of the liquid volume fractions at two ends B.44.

$$\frac{\partial \alpha_{L2}}{\partial y} = \text{constant} \quad (\text{B.44})$$

$$\bar{\alpha}_{L2} = \frac{\alpha_{L,lp} + \alpha_{L,t}}{2} \quad (\text{B.45})$$

The liquid volume fraction at the bottom of the riser ( $\alpha_{L,lp}$ ) is determined by the flow area of the liquid phase at the low-point B.46.

$$\alpha_{L,lp} = \frac{A_L}{\pi r_1^2} \quad (\text{B.46})$$

The liquid volume fraction at the top of the riser is given in equation B.47. This is from an assumption that the liquid volume fraction at the middle of the riser is equal to the average volume fraction in the riser.

$$\alpha_{L,t} = 2\bar{\alpha}_{L2} - \alpha_{L,lp} = \frac{2m_{L2}}{V_2\rho_L} - \frac{A_L}{\pi r_1^2} \quad (\text{B.47})$$

## C Steady state gain

The steady state gain for inlet pressure, topside pressure, mass flow rate and volumetric flow rate ( $P_1$ ,  $P_2$ ,  $W$  and  $Q$ ) is given in table C.1.

Table C.1: Steady state gain

Choke valve opening (Z) [%]	$P_1$ (inlet pressure)	$P_2$ (topside pressure)	W	Q
3	26,0570	24,5945	6,6917E-14	2,3788
4	16,6359	14,6689	1,2610E-14	1,7033
5	10,3854	9,7109	5,6805E-15	1,2401
7	5,0080	5,1270	2,9849E-15	0,7162
10	2,7561	2,5641	6,3830E-15	0,3768
15	1,2406	1,1530	1,9278E-15	0,1743
20	0,7010	0,6513	4,7163E-16	0,0994
30	0,3126	0,2903	5,3076E-16	0,0446
50	0,1127	0,1047	1,9807E-16	0,0162
70	0,0247	0,0229	3,5423E-16	0,0035

## D Kalman filter

The Kalman filter used in the project is the function kalman.m in MATLAB, information about this function is found by typing "help kalman" in MATLAB. This was done for a continuous time estimation. First a continuous plant is given in two equations, where the first one is the state equation D.1 and the second one is the measurement equation D.2.

$$x' = Ax + Bu + Gw \quad (D.1)$$

$$y = Cx + Du + Hw + v \quad (D.2)$$

Here w is process white noise and v is white measurement noise and both these have to satisfy the requirements given in D.3.

$$E(w) = E(v) = 0, E(vw^T) = Q, E(vv^T) = R, E(w, v^T) = N \quad (D.3)$$

A state estimate  $\hat{x}(t)$  is used to minimize the steady state error covariance (D.4), and the optimal solution is the Kalman filter with the equations D.5.

$$P = \lim_{t \rightarrow \infty} E([x - \hat{x}][x - \hat{x}]^T) \quad (D.4)$$

$$\begin{aligned} \hat{x}' &= A\hat{x} + Bu + L(y - C\hat{x} - Du) \\ \begin{bmatrix} \hat{y} \\ \hat{x} \end{bmatrix} &= \begin{bmatrix} C \\ I \end{bmatrix} \hat{x} + \begin{bmatrix} D \\ 0 \end{bmatrix} u \end{aligned} \quad (D.5)$$

The filter gain L in the Kalman filter is determined by solving an Riccati equation D.6. Here P solves the corresponding Riccati equation.

$$L = (PC^T + \bar{N})\bar{R}^{-1} \quad (D.6)$$

where

$$\begin{aligned} \bar{R} &= R + HN + N^T H^T + HQH^T \\ \bar{N} &= G(QH^T + N) \end{aligned} \quad (D.7)$$

The estimator uses the known inputs u and the measurements y to generate the output ( $\hat{y}$ ) and state estimates ( $\hat{x}$ ). It should be noted that  $\hat{y}$  estimates the true plant output. A quite simple illustration of Kalman filter used in a process is shown in figure D.1.

The Kalman function is easy to use and in this project, [kest,L,P] = kalman(sys,Qn,Rn,Nn,sensors,known), was used. The index vectors sensors and known specify which outputs y of sys are measured and which inputs u are known (deterministic). All other inputs or sys are assumed stochastic. Here known is Z, the manipulated variable. Sensors are change between [2] and [2 3] that gives which controlled variables that are used. For [2] only topside pressure is used and for [2 3] topside pressure and topside flow rate is used. Qn and Rn weighting matrices are already given in the report, and Nn was set to zero.



## E Matlab files

The MATLAB scripts and functions that were used in order to produce the results of this project are attached on the CD-ROM marked E. A list of the file names and descriptions are presented in table E.1.

Table E.1: List of MATLAB Files

File name	Description
controllability1.m	Controllability analysis with method 1
controllability2.m	Controllability analysis with method 2
gmsi.m	Stable phase, minimum phase and minimum stable phase for $G_i$ transfer functions
gmsdij.m	Stable phase, minimum phase and minimum stable phase for $G_{d,ij}$ transfer functions
LQG.m	LQG controller

### E.1 Controllability analysis: Method 1

For method 1, only the MATLAB file for inlet pressure as measurement are given.

```

clc
clear all
warning ('off')
%% **** System Inputs ****
par = v4_new_4d_parameters(); %All parameters defined in one file
z0 = 0.3; % NB!!! CHOKE OPENING
wG_in0 = 0.36;
wL_in0 = 8.64;
global u0;
u0 = [z0;wG_in0;wL_in0];
%% ***** Initializing *****
disp('Initializing ... ')
tic
[x0,y0,par] = v4_new_4d_initialize(u0,par);
toc
disp('Initialization completed. ');
disp('##### ');
%% ***** Linearization *****
[A,B,C,D]=v4_new_4d_linmod_knut(x0,y0,u0,par); %analytical
sys =(ss(A,B,C,D));
set(sys, 'inputname', {'Z', 'wG_in', 'wL_in'}, 'outputname', {'P1', 'P2', 'Q'}, 'statename', {'m_G1', 'm_L1↔', 'm_G2', 'm_L2'});
Gu = tf(sys({'P1', 'P2', 'Q'}, 'Z'));
Gd = tf(sys({'P1', 'P2', 'Q'}, {'wG_in', 'wL_in'}));
%% **** Scaling ****
%y output( P1,P2,W)
%d disturbance(wG_in, wL_in)
%u input (Z)

```

```

De=(diag([1 1 1]));
Dd=(diag([0.04 1]));
Du=min(z0,1-z0);

Gu=(De^-1)*Gu*Du;
Gd=(De^-1)*Gd*Dd;
set(Gu, 'inputname', 'Z', 'outputname', {'P1', 'P2', 'Q'});
set(Gd, 'inputname', {'wG_in', 'wL_in'}, 'outputname', {'P1', 'P2', 'Q'});

%% ****Tranfer function and steady state values ****

G1 =Gu('P1', 'Z');
G10 = abs(freqresp(G1,0));
Gd11=(Gd('P1', 'wG_in')); Gd12=(Gd('P1', 'wL_in'));

disp('poles:')
p=pole(G1);
disp(p)
disp('zeros of P1:')
z1=zero(G1);
disp(z1)

%% *** Split G into stable , minimum and stable minimum parts***
ztot=zero(G1); ptot=pole(G1);
z=ztot(find(ztot>0)); p=ptot(find(ptot>0));
nz=length(z); np=length(p);

[Gs1 Gm1 Gms1]=gms1(G1);
[Gds11 Gdm11 Gdms11]=gmsd11(Gd11);
[Gds12 Gdm12 Gdms12]=gmsd12(Gd12);

%% CONTROLLABILITY ANALYSIS FOR P1**
%FIRST FOR P1
%Finding Mpzi and Mzpi
if nz==0 | np==0
    Mpzi=1;
    Mzpi=1;
else
    for i=1:nz
        s=zeros(np,1);
        for j=1:np
            s(j)=abs((z(i)+p(j)))/abs((z(i)-p(j)));
        end
        Mpzi(i)=prod(s);
    end
    Mpzi=max(Mpzi);

    for i=1:np
        t=zeros(nz,1);
        for j=1:nz
            t(j)=abs((z(j)+p(i)))/abs((z(j)-p(i)));
        end
        Mzpi(i)=prod(t);
    end
end

```

```

    Mzpi=max(Mzpi);
end

%bounds
STmin1=max([Mzpi Mpzi]);
SG1=zeros(1,nz);
for i=1:nz
    SG1(i)=abs(evalfr(Gm1,(z(i))));
end
if isempty(SG1)==1
    SGmin1=0;
else
    SGmin1=max(SG1);
end

KS1=zeros(1,np);
for i=1:np
    KS1(i)=abs(evalfr(inv(Gs1),(p(i))));
end

if isempty(KS1)==1
    KSmin1=0;
else
    KSmin1=max(KS1);
end

%First for disturbance 1
SGd11=zeros(1,nz);
for i=1:nz
    SGd11(i)=Mpzi*abs(evalfr(Gdms11,(z(i))));
end
if isempty(SGd11)==1
    SGdmin11=0;
else
    SGdmin11=max(SGd11);
end

KSGd11=zeros(1,np);
for i=1:np
    KSGd11(i)=abs((evalfr(inv(Gs1),(p(i))))*evalfr(Gdms11,p(i)));
end
if isempty(KSGd11)==1
    KSGdmin11=0;
else
    KSGdmin11=max(KSGd11);
end

%For disturbance 2
SGd12=zeros(1,nz);
for i=1:nz
    SGd12(i)=Mpzi*abs(evalfr(Gdms12,(z(i))));
end

```

```

if isempty(SGd12)==1
    SGdmin12=0;
else
    SGdmin12=max(SGd12);
end

KSGd12=zeros(1,np);
for i=1:np
    KSGd12(i)=abs((evalfr(inv(Gs1),(p(i))))*evalfr(Gdms12,p(i)));
end
if isempty(KSGd12)==1
    KSGdmin12=0;
else
    KSGdmin12=max(KSGd12);
end

disp(['The lowest achivable peak for Msmin1 is: ', num2str(STmin1)]);
disp(['The bound for KSmin1 is: ', num2str(KSmin1)]);
disp(['The bound for KSd11 is: ', num2str(KSGdmin11)]);
disp(['The bound for KSd12 is: ', num2str(KSGdmin12)]);
disp(['The bound for SGmin1 is: ', num2str(SGmin1)]);
disp(['The bound for SGdmin11 is: ', num2str(SGdmin11)]);
disp(['The bound for SGdmin12 is: ', num2str(SGdmin12)]);

```

## E.2 Controllability analysis: Method 2

```

clc
clear all
warning ('off')

%% **** System Inputs ****
par = v4_new_4d_parameters(); %All parameters defined in one file
z0 =0.10; % NB!!! CHOKE OPENING
wG_in0 = 0.36;
wL_in0 = 8.64;
global u0;
u0 = [z0;wG_in0;wL_in0];
%% ***** Initializing *****
disp('Initializing ... ')
tic
[x0,y0,par] = v4_new_4d_initialize(u0,par);
toc
disp('Initialization completed. ');
disp('#####');
%% ***** Linearization *****
%With this file it is possible to do the linearization with three different
%methods. Analytical, numerical and by using linmod in matlab.

%options = [0,1e-5,1e-5,1e-12,0,0,0,0,0,0,0,0,0,1e4];
%x,u,y,dx,options] = trim('v4_New_4D_mdl',x0,u0,y0,[],[],[],[],options);

```

```

%para = [1e-5 0 0];
%[A,B,C,D]=linmod('v4_New_4D_mdl',x0,u0,para);
[A,B,C,D]=linmod_knutfunk(x0,y0,u0,par); %analytical
%[A,B,C,D] = v4_new_4d_LinModel_num(x0,y0,u0,par); %numerical
sys =(ss(A,B,C,D));
set(sys,'inputname',{ 'Z','wG_in','wL_in'},'outputname',{ 'P1','P2','W'},'statename',{ 'm_G1','m_L1←
','m_G2','m_L2'});
Gu = tf(sys({'P1','P2','W'},'Z'));
Gd = tf(sys({'P1','P2','W'},{'wG_in','wL_in'}));
%% ****Scaling****
%y output( P1,P2,W)
%d disturbance(wG_in, wL_in)
%u input (Z)
De=(diag([1 1 1]));
Dd=(diag([0.04 1]));
Du=min(z0,1-z0);

Gu=(De^-1)*Gu*Du;
Gd=(De^-1)*Gd*Dd;
set(Gu,'inputname','Z','outputname',{'P1','P2','W'});
set(Gd,'inputname',{'wG_in','wL_in'},'outputname',{'P1','P2','W'});

%% ****Tranfer function and steady state values ****
G1 =(Gu('P1','Z')); G2 =(Gu('P2','Z')); G3 =(Gu('W','Z'));
G10 = abs(freqresp(G1,0)); G20 = abs(freqresp(G2,0)); G30 = abs(freqresp(G3,0)); % steady state ←
value

%Have to have the disturbance matrix Gd for each output,the gas and liquid flow rate into the ←
riser are going
%to be analysed as two separately disturbances.
Gd11=(Gd('P1','wG_in')); Gd12=(Gd('P1','wL_in'));
Gd21=(Gd('P2','wG_in')); Gd22=(Gd('P2','wL_in'));
Gd31=(Gd('W','wG_in')); Gd32=(Gd('W','wL_in'));

%Both G1, G2 and G3 have the same poles.
disp('poles:')
p=pole(G1);
disp(p)
disp('zeros of P1:')
z1=zero(G1);
disp(z1)
disp('zeros of P2:')
z2=zero(G2);
disp(z2)
disp('zeros of W:')
z3=zero(G3);
disp(z3)

z3(end)=0;

%Split G into stable and anti stable part , by using a matlab
%function.
[GSu1, GNSu1]=stabsep(G1,'abstol',1e-5,'reitol',1e-15,'Offset',.01);
[GSu2, GNSu2]=stabsep(G2,'abstol',1e-5,'reitol',1e-15,'Offset',.01);

```

```

[GSu3, GNSu3]=stabsep(G3, 'abstol', 1e-5, 'reltol', 1e-15, 'Offset', .01);

% Stable phase, minimum phase and minimum stable phase of all TF, Functions
% are made to performed this.
[Gs1 Gm1 Gms1]=gms1(G1);
[Gs2 Gm2 Gms2]=gms2(G2);
[Gs3 Gm3 Gms3]=gms3(G3);
[Gds11 Gdm11 Gdms11]=gmsd11(Gd11);
[Gds12 Gdm12 Gdms12]=gmsd12(Gd12);
[Gds21 Gdm21 Gdms21]=gmsd21(Gd21);
[Gds22 Gdm22 Gdms22]=gmsd22(Gd22);
[Gds31 Gdm31 Gdms31]=gmsd31(Gd31);
[Gds32 Gdm32 Gdms32]=gmsd32(Gd32);

%% ***** Controllability analysis*****
%*** Sensitivity and complementary sensitivity peak***
% Sensitivity peak for G1.
[p, z1]=pzmap(G1);
RHPp1=p(find(p>0));
RHPz1=z1(find(z1>0));

if length(RHPp1)>0 && length(RHPz1)>0
np1=length(RHPp1); nz1=length(RHPz1);
sys1=ss(G1); [V,E]=eig(sys1.A); C=sys1.C*V;
for i=1:np1
    Yp(:,i)=C(:,i)/norm(C(:,i)); %Pole direction
end
for i=1:nz1
    [U,S,V]=svd(evalfr(sys1,RHPz1(i))); Yz(:,i)=U(:,end); %zero direction
end
Qp1=(Yp'*Yp).*(1./(diag(RHPp1')*ones(np1)+ones(np1)*diag(RHPp1)));
Qz1=(Yz'*Yz).*(1./(diag(RHPz1)*ones(nz1)+ones(nz1)*diag(RHPz1')));
Qzp1=(Yz'*Yp).*(1./(diag(RHPz1)*ones(nz1,np1)-ones(nz1,np1)*diag(RHPp1)));

Msmn1=sqrt(1+norm(sqrtm(inv(Qz1))*Qzp1*sqrtm(inv(Qp1)))^2);

else
    Msmn1=1;
end

% Sensitivity peak for G2
[p, z2]=pzmap(G2);
RHPp2=p(find(p>0));
RHPz2=z2(find(z2>0));

if length(RHPp2)>0 && length(RHPz2)>0
np2=length(RHPp2); nz2=length(RHPz2);
G2=ss(G2); [V,E]=eig(G2.A); C=G2.C*V;
for j=1:np2
    Yp(:,j)=C(:,j)/norm(C(:,j)); %Pole direction
end
for i=1:nz2
    [U,S,V]=svd(evalfr(G2,RHPz2(i))); Yz(:,i)=U(:,end); %zero direction
end

```

```

Qp2=(Yp'*Yp).*(1./(diag(RHPp2')*ones(np2)+ones(np2)*diag(RHPp2)));
Qz2=(Yz'*Yz).*(1./(diag(RHPz2)*ones(nz2)+ones(nz2)*diag(RHPz2')));
Qzp2=(Yz'*Yp).*(1./(diag(RHPz2)*ones(nz2,np2)-ones(nz2,np2)*diag(RHPp2)));
Msmi2=sqrt(1+norm((Qz2^(-0.5))*Qzp2*(Qp2^(-0.5)))^2);

else
    Msmi2=1;
end

%Sensitivity peak for G3
[p, z3]=pzmap(G3);
z3(end)=0;
RHPp3=p(find(p>0));
RHPz3=z3(find(z3>0));

if length(RHPp3)>0 && length(RHPz3)>0

np3=length(RHPp3); nz3=length(RHPz3);
sys3=ss(G3); [V,E]=eig(sys3.A); C=sys3.C*V;
for i=1:np3
    Yp3(:,i)=C(:,i)/norm(C(:,i)); %Pole direction
end
for i=1:nz3
    [U,S,V]=svd(evalfr(sys3,RHPz3(i))); Yz3(:,i)=U(:,end); %zero direction
end
Qp3=(Yp3'*Yp3).*(1./(diag(RHPp3')*ones(np3)+ones(np3)*diag(RHPp3)));
Qz3=(Yz3'*Yz3).*(1./(diag(RHPz3)*ones(nz3)+ones(nz3)*diag(RHPz3')));
Qzp3=(Yz3'*Yp3).*(1./(diag(RHPz3)*ones(nz3,np3)-ones(nz3,np3)*diag(RHPp3)));

Msmi3=sqrt(1+norm(sqrtm(inv(Qz3))*Qzp3*sqrtm(inv(Qp3)))^2);

else
    Msmi3=1;
end

%% ***KS ****
s=tf('s');
%To find the bound for KS the mirror image of the antistable part of the
%G's are used. If a zero is very close to be negativ, this zero will be
%implemented in the antistable part.

%Lower bound on KS for the output P1
tf=(GNSu1)';
h1=hsvd(tf);
KSmin1=1/min(h1);

%Lower bound on KS for the output P2
tf2=(GNSu2)';
h2=hsvd(tf2);
KSmin2=1/min(h2);

%Lower bound on KS for the output W
tf3=(GNSu3)';
h3=hsvd(tf3);

```

```

KSmin3=1/min(h3);

%% *** KSGd ****
%There are two disturbances for each output, and they will be considered
%separately. d1=wG_in and d2=wL_in

%Lower bound on KSGd1 for the output P1
solve1=((inv(Gdms11))*G1);
[t11s t11ns]=stabsep(solve1);
tfKSd11=(t11ns)';
h4=hsvd(tfKSd11);
KSGd11=1/min(h4);

%Lower bound on KSGd2 for the output P1
solve2=((inv(Gdms12))*G1);
[t12s t12ns]=stabsep(solve2);
tfKSd12=(t12ns)';
h5=hsvd(tfKSd12);
KSGd12=1/min(h5);
%
%Lower bound on KSGd1 for the output P2
solve3=((inv(Gdms21))*G2); %Put in one stable zero, so stabsep works
[t21s t21ns]=stabsep(solve3);
tfKSd21=(t21ns)';
h6=hsvd(tfKSd21);
KSGd21=1/min(h6);

%Lower bound on KSGd2 for the output P2
solve4=((inv(Gdms22))*G2);
[t22s t22ns]=stabsep(solve4);
tfKSd22=(t22ns)';
h7=hsvd(tfKSd22);
KSGd22=1/min(h7);

%Lower bound on KSGd1 for the output W
solve5=((inv((Gdms31)*(1.e-2*s+1)*(1.e-2*s+1)))*G3);
[t31s t31ns]=stabsep(solve5);
tfKSd31=(t31ns)';
h8=hsvd(tfKSd31);
KSGd31=1/min(h8);
%
%Lower bound on KSGd2 for the output W
solve6=((inv((Gdms32)*(1.e-2*s+1))*G3));
[t32s t32ns]=stabsep(solve6);
tfKSd32=(t32ns)';
h9=hsvd(tfKSd32);
KSGd32=1/min(h9);

%% SG *****
%Used the poles and zeros that made the highest bound, since this bound is
%only tight for one RHP-pole and one RHP-zero.
%SG for P1
[p, z1]=pzmap(G1);
RHPp1=p(find(p>0));

```

```

RHPz1=z1(find(z1>0));

if length(RHPp1)>0 && length(RHPz1)>0
np1=length(RHPp1); nz1=length(RHPz1);
sys1=ss(G1); [V,E]=eig(sys1.A); C=sys1.C*V;
for i=1:np1
    Yp(:,i)=C(:,i)/norm(C(:,i)); %Pole direction
end
    for i=1:nz1
        [U,S,V]=svd(evalfr(sys1,RHPz1(i))); Yz(:,i)=U(:,end); %zero direction
    end

num1=abs((Yz'*(evalfr(Gms1,RHPz1(1))))*((evalfr(Gms1,RHPp1(1)))^(-1))*Yp);
den1=norm(Yz'*(evalfr(Gms1,RHPz2(1))),2)*norm(((evalfr(Gms1,RHPp1(1)))^(-1))*Yp,2);
cos1=(num1/den1)^2;
sin1=1-cos1;

term1 = (abs(RHPz1(1)+conj(RHPp1(1))))^2/(abs(RHPz1(1)-RHPp1(1)))^2;
SGmin1=norm((Yz'*(evalfr(Gms1,RHPz1(1)))) ,2)*sqrt(sin1+(term1*cos1)) ;

else
    SGmin1=0;
end

% SG for P2
[p, z2]=pzmap(G2);
RHPp2=p(find(p>0));
RHPz2=z2(find(z2>0));

if length(RHPp2)>0 && length(RHPz2)>0
np2=length(RHPp2); nz2=length(RHPz2);
G2=ss(G2); [V,E]=eig(G2.A); C=G2.C*V;
for j=1:np2
    Yp(:,j)=C(:,j)/norm(C(:,j)); %Pole direction
end

for i=1:nz2
    [U,S,V]=svd(evalfr(G2,RHPz2(i))); Yz(:,i)=U(:,end); %zero direction
end
num2=abs((Yz'*(evalfr(Gms2,RHPz2(2))))*((evalfr(Gms2,RHPp2(2)))^(-1))*Yp);
den2=norm(Yz'*(evalfr(Gms2,RHPz2(2))),2)*norm(((evalfr(Gms2,RHPp2(2)))^(-1))*Yp,2);
cos2=(num2/den2)^2;
sin2=1-cos2;

term1 = (abs(RHPz2(2)+conj(RHPp2(2))))^2/(abs(RHPz2(2)-RHPp2(2)))^2;
SGmin2=norm((Yz'*(evalfr(Gms2,RHPz2(2)))) ,2)*sqrt(sin2+(term1*cos2));
else
    SGmin2=0;
end

% SG for W
[p3, z3]=pzmap(G3);
z3(end)=0;

```

```

RHPp3=p(find(p>0));
RHPz3=z3(find(z3>0));

if length(RHPp3)>0 && length(RHPz3)>0
np3=length(RHPp3); nz3=length(RHPz3);
G3=ss(G3); [V,E]=eig(G3.A); C=G3.C*V;
for j=1:np3
    Yp(:,j)=C(:,j)/norm(C(:,j)); %Pole direction
end

for i=1:nz3
    [U,S,V]=svd(evalfr(G3,RHPz3(i))); Yz(:,i)=U(:,end); %zero direction
end
num3=abs((Yz'*(evalfr(Gms3,RHPz3(1))))*((evalfr(Gms3,RHPp3(1)))^-1)*Yp);
den3=norm(Yz'*(evalfr(Gms3,RHPz3(1))),2)*norm(((evalfr(Gms3,RHPp3(1)))^-1)*Yp,2);
cos3=(num3/den3)^2;
sin3=1-cos3;

term1 = (abs(RHPz3(1)+conj(RHPp3(1))))^2/(abs(RHPz3(1)-RHPp3(1)))^2;
SGmin3=norm((Yz'*(evalfr(Gms3,RHPz3(1)))) ,2)*sqrt(sin3+(term1*cos3));
else
    SGmin3=0;
end

%% ***** SGd *****
%SGd11
[p, z1]=pzmap(G1);
RHPp1=p(find(p>0));
RHPz1=z1(find(z1>0));

if length(RHPp1)>0 && length(RHPz1)>0
np1=length(RHPp1); nz1=length(RHPz1);
sys1=ss(G1); [V,E]=eig(sys1.A); C=sys1.C*V;
for i=1:np1
    Yp(:,i)=C(:,i)/norm(C(:,i)); %Pole direction
end
for i=1:nz1
    [U,S,V]=svd(evalfr(sys1,RHPz1(i))); Yz(:,i)=U(:,end); %zero direction
end

num1=abs((Yz'*(evalfr(Gdms11,RHPz1(2))))*((evalfr(Gdms11,RHPp1(2)))^-1)*Yp);
den1=norm(Yz'*(evalfr(Gdms11,RHPz1(2))),2)*norm(((evalfr(Gdms11,RHPp1(2)))^-1)*Yp,2);
cos1=(num1/den1)^2;
sin1=1-cos1;

term1 = (abs(RHPz1(2)+conj(RHPp1(2))))^2/(abs(RHPz1(2)-RHPp1(2)))^2;
SGdmin11=norm((Yz'*(evalfr(Gdms11,RHPz1(2)))) ,2)*sqrt(sin1+(term1*cos1)) ;

else
    SGdmin11=0;
end

%SGdmin12

```

```

[p, z1]=pzmap(G1);
RHPp1=p(find(p>0));
RHPz1=z1(find(z1>0));

if length(RHPp1)>0 && length(RHPz1)>0
np1=length(RHPp1); nz1=length(RHPz1);
sys1=ss(G1); [V,E]=eig(sys1.A); C=sys1.C*V;
for i=1:np1
    Yp(:,i)=C(:,i)/norm(C(:,i)); %Pole direction
end
    for i=1:nz1
        [U,S,V]=svd(evalfr(sys1,RHPz1(i))); Yz(:,i)=U(:,end); %zero direction
    end

num1=abs((Yz'*(evalfr(Gdms12,RHPz1(2))))*((evalfr(Gdms12,RHPp1(2)))^-1)*Yp);
den1=norm(Yz'*(evalfr(Gdms12,RHPz1(2))),2)*norm(((evalfr(Gdms12,RHPp1(2)))^-1)*Yp,2);
cos1=(num1/den1)^2;
sin1=1-cos1;

term1 = (abs(RHPz1(2)+conj(RHPp1(2))))^2/(abs(RHPz1(2)-RHPp1(2)))^2;
SGdmin12=norm((Yz'*evalfr(Gdms12,RHPz1(2))),2)*sqrt(sin1+(term1*cos1)) ;

else
    SGdmin12=0;
end

%SGdmin21
[p, z2]=pzmap(G2);
RHPp2=p(find(p>0));
RHPz2=z2(find(z2>0));

if length(RHPp2)>0 && length(RHPz2)>0
np2=length(RHPp2); nz2=length(RHPz2);
G2=ss(G2); [V,E]=eig(G2.A); C=G2.C*V;
for j=1:np2
    Yp(:,j)=C(:,j)/norm(C(:,j)); %Pole direction
end
    for i=1:nz2
        [U,S,V]=svd(evalfr(G2,RHPz2(i))); Yz(:,i)=U(:,end); %zero direction
    end
num2=abs((Yz'*(evalfr(Gdms21,RHPz2(2))))*((evalfr(Gdms21,RHPp2(2)))^-1)*Yp);
den2=norm(Yz'*(evalfr(Gdms21,RHPz2(2))),2)*norm(((evalfr(Gdms21,RHPp2(2)))^-1)*Yp,2);
cos2=(num2/den2)^2;
sin2=1-cos2;

term1 = (abs(RHPz2(2)+conj(RHPp2(2))))^2/(abs(RHPz2(2)-RHPp2(2)))^2;
SGdmin21=norm((Yz'*evalfr(Gdms21,RHPz2(2))),2)*sqrt(sin2+(term1*cos2));
else
    SGdmin21=0;
end

%SGdmin22
[p, z2]=pzmap(G2);

```

```

RHPp2=p(find(p>0));
RHPz2=z2(find(z2>0));

if length(RHPp2)>0 && length(RHPz2)>0
np2=length(RHPp2); nz2=length(RHPz2);
G2=ss(G2); [V,E]=eig(G2.A); C=G2.C*V;
for j=1:np2
    Yp(:,j)=C(:,j)/norm(C(:,j)); %Pole direction
end

for i=1:nz2
    [U,S,V]=svd(evalfr(G2,RHPz2(i))); Yz(:,i)=U(:,end); %zero direction
end
num2=abs((Yz'*(evalfr(Gdms22,RHPz2(2))))*((evalfr(Gdms22,RHPp2(2)))^-1)*Yp);
den2=norm(Yz'*(evalfr(Gdms22,RHPz2(2))),2)*norm(((evalfr(Gdms22,RHPp2(2)))^-1)*Yp,2);
cos2=(num2/den2)^2;
sin2=1-cos2;

term1 = (abs(RHPz2(2)+conj(RHPp2(2))))^2/(abs(RHPz2(2)-RHPp2(2)))^2;
SGdmin22=norm((Yz'*(evalfr(Gdms22,RHPz2(2)))) ,2)*sqrt(sin2+(term1*cos2));
else
    SGdmin22=0;
end

%SGdmin31
[p3, z3]=pzmap(G3);
z3(end)=0;
RHPp3=p(find(p>0));
RHPz3=z3(find(z3>0));

if length(RHPp3)>0 && length(RHPz3)>0
np3=length(RHPp3); nz3=length(RHPz3);
G3=ss(G3); [V,E]=eig(G3.A); C=G3.C*V;
for j=1:np3
    Yp(:,j)=C(:,j)/norm(C(:,j)); %Pole direction
end

for i=1:nz3
    [U,S,V]=svd(evalfr(G3,RHPz3(i))); Yz(:,i)=U(:,end); %zero direction
end

num3=abs((Yz'*(evalfr(Gdms31,RHPz3(2))))*((evalfr(Gdms31,RHPp3(2)))^-1)*Yp);
den3=norm(Yz'*(evalfr(Gdms31,RHPz3(2))),2)*norm(((evalfr(Gdms31,RHPp3(2)))^-1)*Yp,2);
cos3=(num3/den3)^2;
sin3=1-cos3;

term1 = (abs(RHPz3(2)+conj(RHPp3(2))))^2/(abs(RHPz3(2)-RHPp3(2)))^2;
SGdmin31=norm((Yz'*(evalfr(Gdms31,RHPz3(2)))) ,2)*sqrt(sin3+(term1*cos3));
else
    SGdmin31=0;
end

%SGdmin32
[p3, z3]=pzmap(G3);

```

```

z3(end)=0;
RHPp3=p(find(p>0));
RHPz3=z3(find(z3>0));

if length(RHPp3)>0 && length(RHPz3)>0
np3=length(RHPp3); nz3=length(RHPz3);
G3=ss(G3); [V,E]=eig(G3.A); C=G3.C*V;
for j=1:np3
    Yp(:,j)=C(:,j)/norm(C(:,j)); %Pole direction
end

for i=1:nz3
    [U,S,V]=svd(evalfr(G3,RHPz3(i))); Yz(:,i)=U(:,end); %zero direction
end

num3=abs((Yz'*(evalfr(Gdms32,RHPz3(2))))*((evalfr(Gdms32,RHPp3(2)))^-1)*Yp);
den3=norm(Yz'*(evalfr(Gdms32,RHPz3(2))),2)*norm(((evalfr(Gdms32,RHPp3(2)))^-1)*Yp,2);
cos3=(num3/den3)^2;
sin3=1-cos3;

term1 = (abs(RHPz3(2)+conj(RHPp3(2))))^2/(abs(RHPz3(2)-RHPp3(2)))^2;
SGdmin32=norm((Yz'*(evalfr(Gdms32,RHPz3(2))),2)*sqrt(sin3+(term1*cos3)));
else
    SGdmin32=0;
end

disp(['The lowest achivable peak for Msmn1 is: ', num2str(Msmn1)]);
disp(['The lowest achivable peak for Msmn2 is: ', num2str(Msmn2)]);
disp(['The lowest achivable peak for Msmn3 is: ', num2str(Msmn3)]);
disp(['The bound for KSmin1 is: ', num2str(KSmin1)]);
disp(['The bound for KSmin2 is: ', num2str(KSmin2)]);
disp(['The bound for KSmin3 is: ', num2str(KSmin3)]);
disp(['The bound for KSGd11 is: ', num2str(KSGd11)]);
disp(['The bound for KSGd12 is: ', num2str(KSGd12)]);
disp(['The bound for KSGd21 is: ', num2str(KSGd21)]);
disp(['The bound for KSGd22 is: ', num2str(KSGd22)]);
disp(['The bound for KSGd31 is: ', num2str(KSGd31)]);
disp(['The bound for KSGd32 is: ', num2str(KSGd32)]);
disp(['The bound for SGmin1 is: ', num2str(SGmin1)]);
disp(['The bound for SGmin2 is: ', num2str(SGmin2(1:1))]);
disp(['The bound for SGmin3 is: ', num2str(SGmin3)]);
disp(['The bound for SGdmin11 is: ', num2str(SGdmin11)]);
disp(['The bound for SGdmin12 is: ', num2str(SGdmin12)]);
disp(['The bound for SGdmin21 is: ', num2str(SGdmin21(1:1))]);
disp(['The bound for SGdmin22 is: ', num2str(SGdmin22(1:1))]);
disp(['The bound for SGdmin31 is: ', num2str(SGdmin31(1:1))]);
disp(['The bound for SGdmin32 is: ', num2str(SGdmin32(1:1))]);

```

## E.2.1 Stable phase, minimum phase and minimum stable phase for $G_i$ transfer functions

This function can be used for all transfer function, by change  $i$  with 1, 2, or 3. This function is made by using [3] at page 176.

```
function [Gsi Gmi Gmsi]=gmsi(Gi)

ztot=zero(Gi); ptot=pole(Gi);
z=ztot(find((ztot>0))); p=ptot(find((ptot>0)));
nz=length(z); np=length(p);

s=TF('s');
b=1;a=1;
for i = 1:np
    b=b*(s-p(i))/(s+p(i));
end;
for i = 1:nz
    a=a*(s+z(i))/(s-z(i));
end

Gsi=minreal(tf(b*G1));Gmi=minreal(tf(G1*a)); Gmsi=minreal(tf(b*G1*a));
```

## E.2.2 Stable phase, minimum phase and minimum stable phase $G_{d,ij}$ transfer functions

This function can be used for all transfer function, by change  $i$  with 1, 2, or 3 and  $j$  with 1 and 2. This function is made by using [3] at page 176. The disturbance is the inlet feed, where it is split in two, considering as two disturbances. The first disturbance is  $w_{G,in}$  and the second disturbance is  $w_{L,in}$ .

```
function [Gdsij Gdmij Gdmsij]=gmsdij(Gdij)

ztot=zero(Gdij); ptot=pole(Gdij);
z=ztot(find(ztot>0)); p=ptot(find(ptot>0));
nz=length(z); np=length(p);

s=TF('s');
b=1;a=1;
for i = 1:np
    b=b*(s-p(i))/(s+p(i));
end;
for i = 1:nz
    a11=a*(s+z(i))/(s-z(i));
end

Gdsij=minreal(tf(b*Gd11));Gdmij=minreal(tf(Gd11*a)); Gdmsij=minreal(tf(b*Gd11*a));
```

### E.3 LQG controller

This files shows how the *Kalman.m* and *lqr.m* function was used. In this file the Kalman filter is based on topside pressure and volumetric flow.

```
%% ** Kalman**
%Kalman filter based on P2 and Q as measured variables.
D1=D(:,1);
D2=D(:,2:3);
Bk=B(:,1);
Bdk=B(:,2:3);
sysk=ss(A,[Bk Bdk],C,[D1 D2], 'inputname', {'Z', 'wG_in', 'wL_in'}, 'outputname', {'P1', 'P2', 'Q'}, '←
state name', {'m_G1', 'm_L1', 'm_G2', 'm_L2'});
sensors = [2 3];
known=[1];
QN=0.02*eye(2); % Standard deviation in measurements
RN=0.02*eye(2); %Inputs uncertainty
NN=0;
[kest, L, P, M, Q] = kalman(sysk, QN, RN, NN, sensors, known)

%% ***LQG***
Qn=eye(4)*1; Rn=1*1000000; N=0;
%Qn=eye(4)*0.1; Rn=1*1000000; N=0;
[lqrk, S, e]=LQR(A, Bk, Qn, Rn, N)
```

## **F Risk evaluation**